EFFECTS OF CYLINDER LOCATION AND SIZE ON MHD NATURAL CONVECTION FLOW IN A SQUARE CAVITY

By

Mohammad Abdur Rob
Student No. 0411093006 P
Registration No. 0411093006, Session: April-2011

MASTER OF PHILOSOPHY
IN
MATHEMATICS

Department of Mathematics
Bangladesh University of Engineering and Technology
(BUET), Dhaka-1000
January - 2019

The thesis titled

EFFECTS OF CYLINDER LOCATION AND SIZE ON MHD NATURAL CONVECTION FLOW IN A SQUARE CAVITY

Submitted by

Mohammad Abdur Rob

Student No. 0411093006 P, Registration No. 0411093006, Session: April-2011, a part time student of M. Phil. (Mathematics) has been accepted as satisfactory in partial fulfillment for the degree of **Master of Philosophy in Mathematics** on January 27, 2019.

BOARD OF EXAMINERS

1. A. Alim
Dr. Md. Abdul Alim — Chairman (Supervisor)
Professor
Dept. of Mathematics, BUET, Dhaka-1000

2.
Head
Prof. Dr. Mustafizur Rahman — Member (Ex-Officio)
Dept. of Mathematics
BUET, Dhaka-1000

3.
Dr. Khandker Farid Uddin Ahmed — Member
Professor
Dept. of Mathematics, BUET, Dhaka-1000

4.
Dr. Rehena Nasrin — Member
Professor
Dept. of Mathematics, BUET, Dhaka-1000

5.
Dr. Md. Mahmud Alam — Member (External)
Professor
Department of Mathematics
Dhaka University of Engineering and Technology (DUET)
Gazipur-1700

CANDIDATE'S DECLARATION

It is hereby declared that this thesis or any part of it has not been submitted elsewhere for the award of any degree or diploma.

(Mohammad Abdur Rob)
Date: 27 January, 2019

DEDICATION

Every challenging work needs self efforts as well as guidence of elders especially those who were very close to our heart. My humble effort I dedicate to

My Mother (late)

who taught me to trust in Allah, encouraging me to believe in myself and hard work.

ACKNOWLEDGEMENT

In the name of Allah, the Most Merciful, the Most Kind. All praises for Almighty Allah, Whose uniqueness, oneness and wholeness is unchallengeable and without His help no work would have been possible to reach the goal. First and foremost, I have to thank my thesis supervisor, Dr. Md. Abdul Alim, Professor, Department of Mathematics, Bangladesh University of Engineering and Technology (BUET). Without his assistance and dedicated involvement in every step throughout the process, this paper would have never been accomplished. I would like to thank you very much for your support and understanding over the past five years.

I am thankful from the core of my heart to Prof. Dr. Md. Mustafizur Rahman, Head, Department of Mathematics, Prof. Dr. Khandker Farid Uddin Ahmed, and Prof. Dr. Rehena Nasrin for their guidance and supports.

I am indebted to the external member of the Board of Examiners, Dr. Md. Mahmud Alam, Professor, Department of Mathematics, Dhaka University of Engineering and Technology (DUET), Gazipur, for his valuable suggestions in upgrading the quality of the work.

My special thanks go to all of my respectable teachers and staffs of the Department of Mathematics, BUET, Dhaka, for their kind help and support.

I am grateful to all of my colleagues of Eastern University and Mr. A K M Reaz Uddin, M. Phil student, Department of Mathematics, BUET, for their encouragement and supporting mentality in all affairs especially in my thesis work.

Finally, I express my devoted affection to my wife Mrs. Bilkis Begum, my beloved daughters Rubaiya Tasnova Rahi, Rubaba Tasnia Mahi and all of my family members and relatives for making a delightful atmosphere as well as excusing me from family duties in order to complete the courses, research studies and final completion of the thesis work.

ABSTRACT

Heat transfer phenomenon in a square cavity with MHD natural convection flow has been over looked numerically. In this research under the title "Effects of cylinder location and size on MHD natural convection flow in a square cavity", two cases have been considered: (I) Variation of cylinder's position vertically keeping size (radius, r) of the cylinder as a constant and (II) Variation of cylinder size (radius, r) keeping cylinder position at (0.50, 0.50) as a constant. The bottom wall of the cavity and the cylinder has kept at high temperature (T_h) and the rest of the walls have remained at low temperature (T_c).

The research has been performed for different values of Rayleigh number (Ra), Hartmann number (Ha), Prandtl number (Pr), physical parameter: size (radius) of the heated cylinder (r) and various position of the heated cylinder. The numerical results have been reported for the effect of buoyancy parameter, Rayleigh number ($10^4 \le Ra \le 5\times10^6$), magnetic field parameter, Hartmann number ($0 \le Ha \le 50$) and the thermal diffusivity parameter, Prandtl number ($0.71 \le Pr \le 10$). Three positions (0.50, 0.25), (0.50, 0.50) and (0.50, 0.75) of the heated cylinder have been considered in the case (I) where the size (radius, r) of the cylinder has maintained as a constant (r = 0.20 m). Besides, in case (II), the size (radius, r) of the heated cylinder has been altered from r = 0.10 to 0.30 m keeping cylinder position at (0.50, 0.50) as a constant.

The strength of the velocity magnitude has been improved for both cases with the increase of Rayleigh number (Ra) and Prandtl number (Pr). But the strength of the velocity magnitude has been declined for both cases with the increase of Hartmann number (Ha). The maximum (184 m/s) average velocity magnitude (V_{av}) in the cavity has been observed when cylinder size, r = 0.30 m, CP at (0.50, 0.50), Ra = 5×10^6, Pr = 0.71 and Ha = 50.

Finally, appreciable effects of heat transfer rate have been illustrated for the size variation of the heated cylinder compared to the position variation. Evaluations with earlier published work have been executed and the results have found to be in good agreement.

CONTENTS

NOMENCLATURE

B_0	Magnetic induction
CP	Cylinder's position
C_p	Specific heat at constant pressure (J/kg K)
g	Gravitational acceleration (m/s^2)
h	Convective heat transfer coefficient (W/m^2 K)
Ha	Hartmann number
k	Thermal conductivity of fluid(W/m K)
L	Height or base of square cavity (m)
K	Thermal conductivity ratio fluid
Nu	Local Nusselt number
Nu_{av}	Average Nusselt number
P	Non-dimensional pressure
p	Pressure
Pr	Prandtl number
r	Radius of the heated cylinder
Ra	Rayleigh number
T	Dimensional temperature (K)
U	x component of dimensionless velocity
u	x component of velocity (m/s)
V	y component of dimensionless velocity
V_{av}	Average velocity magnitude (m/s)
v	y component of velocity (m/s)
x, y	Cartesian coordinates
X, Y	Dimensionless Cartesian coordinates

Greek symbols

α	Thermal diffusivity (m^2/s)
β	Coefficient of thermal expansion (K^{-1})
ρ	Density of the fluid (kg/m^3)
θ	fluid temperature
μ	dynamic viscosity of the fluid (Pa s)
ν	Kinematic viscosity of the fluid (m^2/s)
σ	Fluid electrical conductivity(Ω^{-1}m^{-1})

Subscript

av	average
h	hot
c	cool

LIST OF TABLES

LIST OF FIGURES

CHAPTER 1

INTRODUCTION

1.1 Preface

Heat and temperature are the most misunderstood concepts of thermodynamics. The idea of heat and temperature are studied together in science theoretically, which is somewhat related but not alike. The terms are very common due to their wide usage in our day to day life. There exists a fine line which separates heat from temperature, in the sense that heat is thought of as a form of energy, but the temperature is a measure of energy. In other words, heat is a transfer of energy from one object to another due to a difference in temperature and it might change the state of temperature. Besides, the temperature is a physical state, based on the molecular activity of an object.

Natural or Buoyant or Free convection is a very important mechanism that is functioning in a variety of environments of nature. It is caused by the action of density gradients in combination with a gravitational field. It is measured in many practical applications such as the energy conservation in buildings, cooling of electronic equipment, cooling of nuclear reactor systems, solar engineering, environmental and geothermal fluid dynamics. These application areas include the cooling of electronic devices, double-pane windows, heating and cooling of building, refrigerators, room ventilation, heat exchangers, solar collectors and so on.

In the past, many investigations have dealt with natural convection from a heated body placed concentrically or eccentrically inside a cooled enclosure. With the invention of stream engine by James watt in 1765, the phenomenon of heat transfer got its first industrial recognition and after that its use extended to a great extent and spread out in different spheres of engineering fields. In the past three decades, digital computers, numerical techniques and development of numerical models of heat transfer have made it possible to calculate heat transfer of considerable complexity and thereby create a new approach to the design of heat transfer equipment.

The study of the universe has led to the realization that all physical phenomenon are subject to natural laws. The term natural might well be used to describe the framework or system of fundamental and universal importance within this system is the mechanisms for the transfer of heat. Heat transfer is a branch of applied thermodynamics. It estimates the rate at which heat is transferred across the system boundaries subject to specific temperature differences and the temperature distribution of the system during the process. Whereas classical thermodynamics deals with the amount of heat transferred during the process. Heat transfer processes have always been an integral part of our environment.

1.2 Keywords

1.2.1 Square Cavity

Square cavity is a two dimensional segment of a cubical solid figure. Its name is square enclosure. For research purpose, the thickness of the cavity is ignored. The square cavity/enclosure is used in the daily life appliance for many purposes.

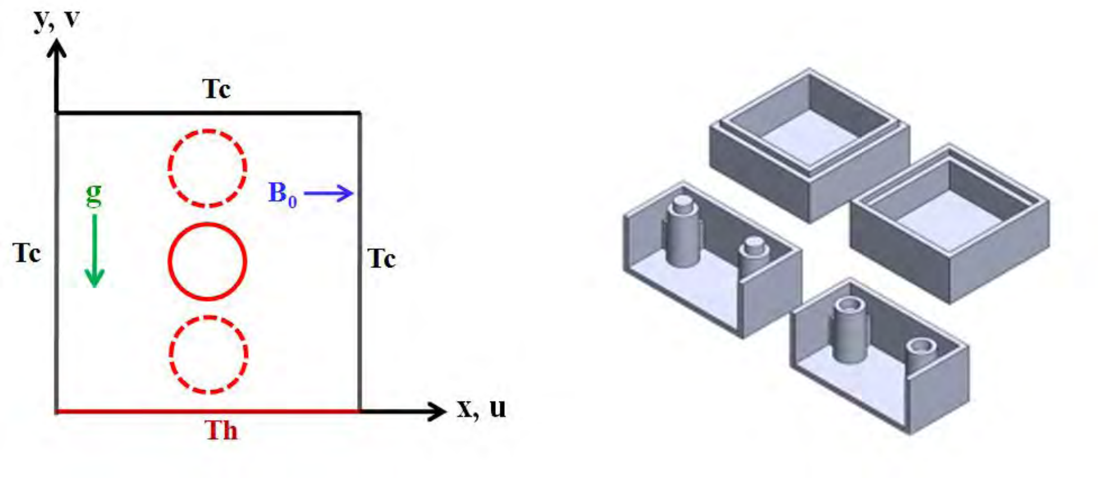

Fig.1.1 (a) 2D square cavity (b) 3D view of square cavity

1.2.2 Magnetohydrodynamics (MHD)

Magnetohydrodynamics is the study of the magnetic properties and behaviour of electrically conducting fluids. Examples of such magneto fluids include plasmas, liquid metals, salt water, and electrolytes. The word "magnetohydrodynamics" is derived from magneto-meaning magnetic field, hydro-meaning water, and dynamics meaning movement. The field of MHD was initiated by Hannes Alfvén, for which he received the Nobel Prize in Physics in 1970. The fundamental concept behind MHD is that magnetic fields can induce currents in a moving conductive fluid, which in turn polarizes the fluid and reciprocally changes the magnetic field itself. The set of equations that describe MHD are a combination of the Navier–Stokes equations of fluid dynamics and Maxwell's equations of electromagnetism. These differential equations must be solved simultaneously, either analytically or numerically. At present, a plenty of energy is needed to sustain industrial and agricultural production. The existing conventional energy sources are not adequate to meet the ever increasing energy demands. To fulfill the additional energy demand, MHD is used for various purposes like astrophysics (planetary magnetic field), jet printers, dispersion (granulation) of metals, MHD pumps, magnetic filtration and separation, ship propulsion, MHD flow meters, MHD generators, MHD flow control (reduction of turbulent drag) etc.

The ideal MHD equations consist of the continuity equation, the momentum equation, and Ampere's Law in the limit of no electric field and no electron diffusivity, and a temperature evolution equation. As with any fluid description to a kinetic system, a closure approximation must be applied to highest moment of the particle distribution equation. This is often accomplished with approximations to the heat flux through a condition of adiabaticity or isothermality. MHD is used in the fields of geophysics, engineering, sensors, astrophysics, magnetic drug targeting etc.

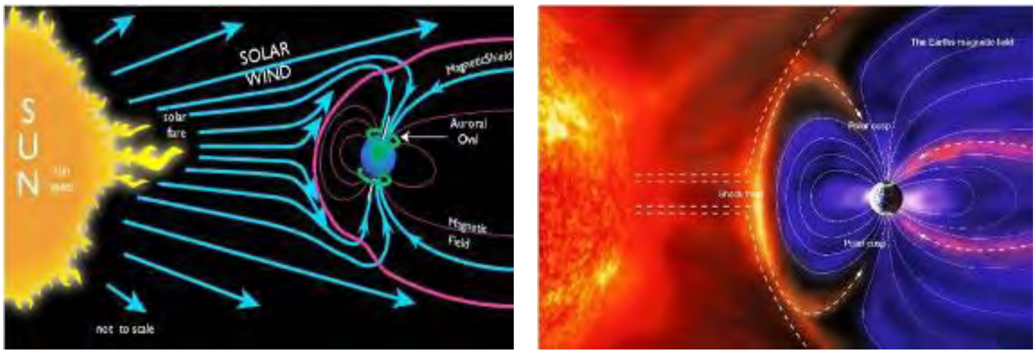

Fig.1.2 The Magnetosphere shields (protect from a danger) the surface of the Earth from the charged particles of the solar wind and is generated by electric currents located in many different parts of the Earth. It is compressed on the day (Sun) side due to the force of the arriving particles, and extended on the night side (Credit: NASA).

1.2.3 Free or Natural Convection

A natural convection flow field is a self-sustained flow driven by the presence of a temperature gradient. It is applicable when there is no external flow exists. It is the loss of heat from a hot solid or liquid into air which is not artificially agitated.

Free convection in enclosures has attracted considerable interest for researchers because of its presence both in nature and engineering applications, for example, multi-pane windows, cooling of electronic equipments, solar thermal design, aircraft housing systems and other equipments.

1.2.4 Stream Function

Stream function is a very useful device in the study of fluid dynamics and was arrived at by the French mathematician Joseph Louis Lagrange in 1781. The idea of introducing stream function works only if the continuity equation is reduced to two terms. If a function $\psi(x, y)$ satisfies the continuity equation $\frac{\partial u}{\partial x} + \frac{\partial u}{\partial y} = 0$, then $\psi(x, y)$ is known as stream function. The relations among stream function $\psi(x, y)$ with velocity components for two-dimensional flows are $u = \frac{\partial \psi}{\partial y}$ and $v = -\frac{\partial \psi}{\partial x}$. The positive sign of $\psi(x, y)$ denotes anti-clockwise circulation and the clockwise circulation is represented by the negative sign of $\psi(x, y)$.

1.2.5 Thermal Conductivity

Thermal conductivity refers to the amount/speed of heat transmitted through a material. Heat transfer occurs at a higher rate across materials of high thermal conductivity than those of low thermal conductivity. Materials of high thermal conductivity are widely used in heat sink applications and materials of low thermal conductivity are used in thermal insulation. Thermal conductivity of materials is temperature dependent. The reciprocal of thermal conductivity is called thermal resistivity. Metals with high thermal conductivity, e.g. copper exhibits high electrical conductivity. The heat generated in high thermal conductivity materials is rapidly conducted away from the region of the weld. For metallic materials, the electrical and thermal conductivity correlate positively, i.e. materials with high electrical conductivity (low electrical resistance) exhibit high thermal conductivity. The proportionality constant *k* is called thermal conductivity of the material. The thermal conductivity *k* is defined by

$$k = \frac{\text{Heat flow (Q)} \times \text{Thickness of the material (L)}}{\text{Surface area of material (A)} \times \text{Temperatur e gradient } (\Delta T)}$$

1.2.6 Thermal Diffusivity

Thermal diffusivity is the rate of transfer of heat of a material from the hot side to the cold side. It can be calculated by taking the thermal conductivity divided by density and specific heat capacity at constant pressure. Thermal diffusivity represents how fast heat diffuses through a material and is defined as

$$\alpha = \frac{k}{\rho c_p}$$

where, k is thermal conductivity [W/(m·K)], ρ is density [kg/m³] and c_p is specific heat capacity [J/(kg·K)]

A material that has a high thermal conductivity or a low heat capacity will obviously have a large thermal diffusivity. The larger thermal diffusivity means that the propagation of heat into the medium is faster. A small value of thermal diffusivity means the material mostly absorbs the heat and a small amount of heat is conducted further.

1.2.7 Incompressible Flow

In fluid dynamics, incompressible flow refers to a flow in which the density remains constant in any fluid packet, i.e. any infinitesimal volume of fluid moving in the flow. This type of flow is also referred to as isochoric flow, from the Greek isos-choros which means “same space/area”. It is important to underline the difference between an “incompressible flow” and an “incompressible fluid”: while the first is a characteristic of the flow, the second is a characteristic of the material. All fluids are apriori compressible but many are considered to be incompressible because the density variation is negligible for common applications. Incompressibility is a feature exhibited by any fluid under certain conditions. The behavior of control volume (CV) for incompressible flow is depicted in the image below. It can be seen that the CV remains constant for a flow that is incompressible

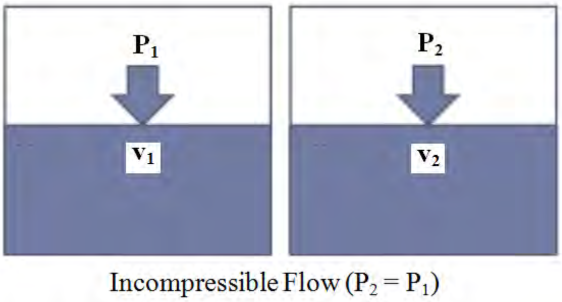

Fig. 1.3 Incompressible flow

1.3 Dimensionless parameters

Dimensionless parameters in fluid mechanics are a set of dimensionless quantities that have an important role in the behaviour of fluids. Mechanical engineers often work with dimensionless numbers**.** These are either pure numbers that have no units or groupings of variables in which the units exactly cancel one another again leaving a pure number. A dimensionless number can be the ratio of two other numbers and in that instance, the dimensions of the numerator and denominator will cancel. The dimensionless parameters can be considered as measures of the relative importance of certain aspects of the flow. Some dimensionless parameters related to the present study are discussed below:

1.3.1 Hartmann Number, Ha

Hartmann number is the ratio of electromagnetic force to the viscous force first introduced by Hartmann. It is defined by

$$\mathrm{Ha} = B_0 L \sqrt{\frac{\sigma}{\mu}}$$

where, B_0 is the magnetic field, L is the characteristic length scale, σ is the electrical conductivity and μ is the dynamic viscosity.

1.3.2 Prandtl Number, Pr

The relative thickness of the velocity and the thermal boundary layers are best described by the dimensionless parameter Prandtl number which is defined as

$$\mathrm{Pr} = \frac{\upsilon}{\alpha} = \frac{\text{Viscous diffusion rate}}{\text{Thermal diffusion rate}} = \frac{c_p \mu}{k}$$

where ν is the kinematic viscosity, $\nu = \frac{\mu}{\rho}$, α is the thermal diffusivity and $\alpha = \frac{k}{(\rho c_p)}$, μ is the dynamic viscosity, k is the thermal conductivity, c_p is the specific heat and ρ is the density. It is named after Ludwing Prandtl, who introduced the concept of boundary layer in 1904 and made significant contributions to boundary layer theory. The Prandtl number of fluids ranges from less than 0.01 for liquid metals to more than 100,000 for heavy oils. Small values of the Prandtl number, $\mathrm{Pr} << 1$, means the thermal diffusivity dominates whereas with large value of Pr ($\mathrm{Pr} >> 1$) means the momentum diffusivity dominates the behavior.

1.3.3 Rayleigh Number, Ra

The Rayleigh number for a fluid is a dimensionless number associated with buoyancy driven flow in fluid mechanics. When the Rayleigh number is below the critical value for that fluid, heat transfer is primarily in the form of conduction. When it exceeds the critical value, heat transfer is primarily in the form of convection. The Rayleigh number is named after Lord Rayleigh and is defined as the product of the Grashof number, which describes the relationship between buoyancy and viscosity within a fluid, and the Prandt number, which describes the relationship between momentum diffusivity and thermal diffusivity. Hence the Rayleigh number itself may also be viewed as the ratio of buoyancy forces and thermal and momentum diffusivities. For convection near a vertical wall, this number is

$$Ra_x = Gr_x Pr = \frac{g\beta}{\nu\alpha}(T_s - T_\infty)x^3$$

where

x = Characteristic length (in this case, the distance from the leading edge)

Ra_x = Rayleigh number at position x

Gr_x = Grashof number at position x

Pr = Prandtl number

g = acceleration due to gravity

T_s = Surface temperature (temperature of the wall)

T_∞ = Quiescent temperature (fluid temperature far from the surface of the object)

ν = Kinematic viscosity

α = Thermal diffusivity

β = Thermal expansion coefficient

For most engineering purposes, the Rayleigh number is large, somewhere around 10^6 and 10^8.

1.4 Literature Review

The fundamental problem of natural convection heat transfer in a square cavity has received a considerable attention from researchers. Magnetohydrodynamic (MHD) natural convection flow in a square cavity with heated cylindrical block has the important industrial applications which have been reported by Zhang *et al.* (2016). Applications include electronic cooling, chemical apparatus, aeronautics, fire research, solar antenna, etc. MHD natural convection heat transfer inside any shaped cavity is not a new dilemma for research. It has drawn the interest of a large number of researchers because of its various applications. Han (2009) investigated numerically the thermal radiation effects on natural convection of an electrically conducting and radiating fluid in a square cavity with an external magnetic field aligned to gravity. The author has found that the radiation was played a significant role. Basak *et al.* (2010) illustrated that Nusselt numbers have almost invariant with Grashof number (Gr) where Prandtl (Pr) number Pr = 0.7 for linearly heated side walls or cooled right wall.

Obayedullah *et al.* (2013) found the temperature, fluid flow and heat transfer strongly depend on internal and external Rayleigh and Hartmann numbers under MHD natural convection flow. Hossain *et al.* (2002) found the thermal gradients reduced near the heated wall on unsteady laminar natural convection flow. Sathiyamoorthy *et al.* (2007) analyzed the minor circulations become weaker for higher Prandtl number fluid. Oztop *et al.* (2011) investigated MHD mixed convection in a lid-driven cavity with corner heater. Hossain *et al.* (2015) illuminated on MHD free convection flow in open square cavity containing heated circular cylinder by finite element analysis based on Galerkin weighted residual approach. The authors have been established that for all cases of Ha and Ra the isothermal lines concentrate to the right lower corner of the cavity and there was a recirculation around the cylinder and one vortex has been created in the flow field.

Jami *et al.* (2008) have found remarkable results on natural convection flow in a square enclosure containing a solid cylinder. Sheikhzadeh *et al.* (2010) examined the effect of length ratio on magneto-convection in a square enclosure with a square block for low Prandtl number fluid. Meanwhile Jani *et al.* (2013) investigated MHD free convection in a square cavity and observed that, for low Rayleigh numbers, by increase in the Hartmann number, free convection suppressed and heat transfer occurred through conduction mainly. Ali *et al.* (2017) investigated MHD free convection flow in a differentially heated square cavity with tilled obstacle and illuminated that the considerable heat transfer enhancement was found for the influenced of higher Rayleigh number and lower Hartmann number and the opposite phenomenon also observed in the case of average temperature.

For MHD free convection and entropy generation in a square porous cavity, the non-dimensional numbers namely, Rayleigh number $(\mathrm{Ra} = 1 - 10^4)$ and Hartmann number $(\mathrm{Ha} = 1 - 10)$ was analyzed by Mahmud and Fraser (2004). A natural convection flow under a magnetic field has shown to influence the heat transfer rate in a rectangular enclosure by Ece and Büyük (2006). Kahveci and Öztuna (2009) have numerically studied in a laterally heated partitioned enclosure with MHD natural convection flow. The authors have been over looked the average heat transfer rate decreases up to 80% if the partition was placed at the midpoint and an x-directional magnetic field was applied. Munshi *et al.* (2015) inquired into the effect of MHD natural convection flow in a square enclosure with an adiabatic obstacle and was found some significant phenomenon on that flow.

Park *et al.* (2014) examined the natural convection flow in a square enclosure with two inner circular cylinders positioned at different vertical locations. The authors have been concluded the natural convection induced by a temperature difference between a cold outer square enclosure and two hot inner circular cylinders for different Rayleigh numbers in the range of $10^3 \le \mathrm{Ra} \le 10^6$. A numerical study of natural convection in a square enclosure was performed with a circular cylinder at different vertical locations by Kim *et al.* (2008). The authors have been over looked the characteristics of a two-dimensional natural convection problem in a cooled square enclosure with an inner heated circular cylinder numerically.

Bakar *et al.* (2016) examined the influence of Hartmann number and the Richardson number on the characteristics of mixed convection heat flow inside a lid-driven square cavity having the top lid moving with uniform speed. Rahman *et al.* (2010) examined the conjugate effect of joule heating and MHD mixed convection in an obstructed lid-driven square cavity by employing Galerkin weighted residual method of finite element. The authors have been claimed that any obstacle made some significant influences on the MHD mixed convection flow. Bouabid *et al.* (2011) studied the contributions of thermal, diffusive, friction and magnetic effects on entropy generation. The authors have been illustrated entropy generation due to heat transfer and then mass transfer. Hamama *et al.* (2016) interpreted irreversibility investigation on MHD natural convection in a square cavity for different Prandtl numbers. The authors have been observed the influence of Prandtl number in presence of a magnetic field on heat transfer, fluid flow and entropy generation in natural convection through a square cavity.

MHD natural convection in a vertical cylindrical cavity with a sinusoidal upper wall temperature has investigated by Kakarantzas *et al.* (2009). The authors have been concluded that the domination of conduction heat transfer was more prominent in the case of an axial magnetic field because of the formation of the Hartmann layer near the upper surface. On the other hand, Javed *et al.* (2018) recapitulated on MHD natural convective flow through a porous medium in a square cavity filled with liquid gallium by Galerkin FEM. The authors have been observed that the Darcy number was increased for both cases: increase of strength of streamline circulations and increase in the height of isotherms in the cavity.

The influence of magnetic field on natural convection inside the enclosures partially filled with conducting square solid obstacles was presented by Ashouri *et al.* (2014). The authors have been clarified on MHD natural convection flow in cavities filled with square solid blocks. Hasanuzzaman *et al.* (2012) examined the effects of MHD natural convection in trapezoidal cavities with different inclination angles. The authors have been scrutinized that heat transfer decreased by 20.70% and 16.15% as φ was increased from 0 to 60 at $Ra = 10^5$ and 10^6 respectively. On the other hand, heat transfer decreased by 20.28% and 13.42% as Ha was increased from 0 to 50 for $Ra = 10^5$ and 10^6 respectively.

Kahveci (2007) carried out the polynomial-based differential quadrature (PDQ) method to simulate the natural convection flow in a partitioned enclosure. The average Nusselt number was decreased towards a constant value as the partition was distanced from the hot wall towards the middle of the enclosure was observed by the author. Sathiyamoorthy and Chamkha (2012) made the effect of magnetic field on natural convection in an enclosure with uniformly or linearly heated adjacent walls and especially its effect on the local and average Nusselt numbers. The authors have been clarified that the presence of a magnetic field causes significant effects on the local and average Nusselt numbers on all considered walls. Rahman *et al.* (2011) examined magnetic field effect on mixed convection in a lid driven cavity and found average Nusselt number was decreased with increase Hartmann number and joule heating parameter.

Jalil *et al.* (2013) investigated natural convection in the cavity with the partial magnetic field at internal $\mathrm{Ra} = 10^7$ and external $\mathrm{Ra} = 10^5$ at $\mathrm{Pr} = 0.024$. The authors have been examined for a given Ha, chaotic fluid flow was tend to become periodic one at particular amplitude and frequency; while high magnetic field strength, the flow in the cavity was tend to become steady laminar with stable average Nusselt number. Kakarantzas *et al.* (2014) explained buoyancy-driven flow under magnetic field between coaxial isothermal cylinders with working fluid as liquid metal by using direct numerical simulation. Electrically conducting free convection in liquid metal filled linearly heated cavity of square shape was investigated by Sathiyamoorthy and Chamkha (2010). The authors have been found that the average Nusselt number of the uniformly heated bottom wall was higher for vertically-applied magnetic field than for horizontally-applied magnetic field for moderate values of Hartmann numbers for both cases of thermal boundary conditions.

Basak *et al.* (2009) analyzed for natural convection within trapezoidal enclosures based on heatline concept. Parametric study for the wide range of Rayleigh number (Ra), $10^3 \le \mathrm{Ra} \le 10^5$ and Prandtl number (Pr), $0.026 \le \mathrm{Pr} \le 1000$ with various tilt angles $\varphi = 45^\circ$, 30° and 0° (square) have been carried out by the authors. Hossain *et al.* (2017) inquired into the effect of Prandtl number (Pr) and inclination angle of the cavity on MHD natural convection heat transfer and fluid flow inside the cavity by visualizing the fluid flow in terms of isotherms and streamlines respectively. Pirmohammadi and Ghassemi (2009) studied the effect of magnetic field on convection heat transfer inside a tilted square enclosure. The authors have been investigated the laminar natural convection flows in the presence of a longitudinal magnetic field in a tilted enclosure that is heated from below and cooled from the top while other walls were adiabatic.

Luo *et al.* (2016) over looked the effects of thermal radiation on MHD flow and heat transfer in a cubic cavity. The authors have been observed that the increasing of Hartmann number, the isothermal surface was considerable changes and the flow structure and isotherm on the different mid-plane of the cubic cavity was changed distinctly. Türk and Sezgin (2013) examined the FEM solution of natural convection flow in square enclosures under magnetic field and have been observed that streamlines formed a thin boundary layer close to the heated walls as Ha was increased. Alam *et al.* (2017) performed finite element analysis of MHD natural convection in a rectangular cavity and partially heated wall. The authors have been viewed that the Hartmann number and Rayleigh number were strong influence on the streamlines and isotherms. Chamkha *et al.* (2011) investigated on the mixed convection from a heated square solid cylinder enclosed in a square air-filled cavity with various geometry configurations. The authors have been studied the effect of the locations of the inner square cylinder and aspect ratio. These effects were found to play significant roles in the streamline and isotherm contour patterns.

Rahman *et al.* (2009) observed MHD mixed convection around a heat conducting horizontal circular cylinder in a rectangular lid-driven cavity with joule heating. The electromagnetic force can be reduced to the damping factor $-B_0\upsilon$, where v was the vertical velocity component. As a result, the Lorentz force depends only on the velocity component perpendicular to the magnetic field. The authors have been concluded that the flow behavior and the heat transfer characteristics inside the cavity were strongly depending upon the strength of the magnetic field. Kim *et al.* (2014) investigated the effect of the variation in the bottom wall temperature on fluid flow and heat transfer in the enclosure with a circular cylinder for different Rayleigh numbers in the range of $10^3 \le \mathrm{Ra} \le 10^6$. The authors have been viewed that for Ra = 10^3, 10^4 and 10^6 the value of $\langle \mathrm{N}_{\mathrm{u}_\mathrm{t}} \rangle$ increased monotonically with increasing θ_b, even though variation of $\langle \mathrm{N}_{\mathrm{u}_\mathrm{t}} \rangle$ according to θ_b was very small for Ra = 10^3 and 10^4. Roslan *et al.* (2014) inquired into natural convection in a differentially heated square enclosure with a solid polygon numerically. The authors have been found the strength of the flow and inner heat circulations was much higher for greater N. The conjugate heat transfer via natural convection and conduction in a triangular enclosure filled with a porous medium investigated by Varol *et al.* (2009). The authors have been found that both thermal conductivity ratio and thickness of the bottom wall was used as control parameters for heat transport and flow field. The authors also have been clarified that the strength became lower for thin wall or low values of thermal conductivity ratio and the value of thermal conductivity parameter k was effective for $k > 1$.

Pirmohammadi *et al.* (2008) examined the effect of a magnetic field on buoyancy-driven convection in differentially heated square cavity and have been illustrated that the imposition of the magnetic field on buoyancy driven circulation system was modified both the velocity and the temperature field. Park *et al.* (2013) have studied on natural convection in a cold square enclosure with a pair of hot horizontal cylinders positioned at different vertical locations by using the immersed boundary technique of a finite volume method. The authors have been found that the profile of $\overline{Nu}_{en}$ along the vertical direction of the cylinder (δ) shown an almost symmetric distribution along the center of the enclosure ($\delta = 0$) for low Rayleigh number ($Ra = 10^3$ or 10^4). Saha (2013) investigated the effect of MHD and heat generation on natural convection flow in an open square cavity under microgravity condition $(g \approx 0)$ and under a uniform vertical gradient magnetic field in an open square cavity with three cold sidewalls. The author has been concluded that the heat transfer rate was suppressed in increased of the magnetic Rayleigh number and the paramagnetic fluid parameter for the present investigation.

Natural convection in rectangular enclosures heated from below and symmetrically cooled from the sides was investigated by Ganzarolli and Milanez (1995) and the flow structure was found to consist of a single counterclockwise cell for all cases studied, except for a small secondary cell due to viscous drag observed in some cases for uniform temperature at the cavity floor. Kherief *et al.* (2016) examined the MHD flow in two dimensional inclined rectangular enclosure heated and cooled on adjacent walls. The authors have been illustrated that the flow characteristics and the convection heat transfer inside the tilted enclosure, depend strongly upon the strength and direction of the magnetic field and the inclination of the enclosure. Aydin *et al.* (1999) presented the results of a numerical study of buoyancy included flow and heat transfer in a two dimensional enclosure isothermally heated from one side and cooled from the ceiling. The authors have been observed that the effect of Rayleigh number (Ra) on heat transfer has significant more when the enclosure is shallow.

1.5 Main Objectives of the Present Study

The aim of the study is to investigate the effects of heat flow mathematically and numerically for MHD free convection in a square cavity in the presence of heated cylinder. In this research, two cases have been considered: (I) Variation of cylinder’s position in the square cavity and (II) Variation of cylinder’s size (radius) where cylinder is kept at the centre of the square cavity. Results are presented in terms of streamlines, isotherms, average Nusselt number, average fluid temperature, average velocity magnitude and related graphs and charts. However, the main objectives of the research are as follows:

i) To solve the mathematical model using weighted residual Finite Element Method (FEM).
ii) To examine the effects of various parameters such as Rayleigh number (Ra), Hartmann number (Ha) and Prandtl number (Pr).
iii) To investigate the variations of the heat transfer rate, average Nusselt number, average fluid temperature and average velocity magnitude inside the cavity.
iv) To compare results with other published works.
v) To make an optimum combination of the aforesaid parameters.

1.6 Outline of the Thesis

This thesis contains four chapters. It is concerned with the analysis of heat transfer rate for MHD free convection in a square cavity with a heated cylinder.

In Chapter 1, a brief introduction is presented with aim and objective. Some non-dimensional parameters have explained here. Some literature review of the past studies on fluid flow and heat transfer in cavities or channels have also been illustrated in this chapter.

The physical and mathematical model along with the computational procedure of the problem is explained in Chapter 2.

In Chapter 3, a detailed results and discussion with figures and tables have been performed for different cases.

Finally, in Chapter 4, the dissertation has been rounded off with the conclusions and a recommendation for further study of the present problem is summarized.

CHAPTER 2

MATHEMATICAL & NUMERICAL MODELING

2.1 Mathematical Modeling

The convection heat transfer occurs due to temperature differences which affect the density, and thus relative buoyancy of the fluid is referred to as free convection (natural convection). The starting point of any numerical method is the mathematical model, i.e. the set of partial differential equations and boundary conditions. A solution method is usually designed for a particular set of equations. Trying to produce a general-purpose solution method, i.e. one which is applicable to all flows, is impractical, is not impossible and as with most general purpose tools, they are usually not optimum for any one application.

The generalized governing equations are used based on the conservation laws of mass, momentum and energy. As the heat transfer depends upon a number of factors, a dimensional analysis is presented to show the important non-dimensional parameters which will influence the dimensionless heat transfer parameter, i.e. Nusselt number.

2.2 Algorithm

The algorithm was originally put forward by the iterative Newton-Raphson algorithm; the discrete forms of the continuity, momentum and energy equations are solved to find out the value of the velocity and the temperature. It is essential to guess the initial values of the variables. Then the numerical solutions of the variables are obtained while the convergent criterion is fulfilled. The simple algorithm is shown by the following flow chart.

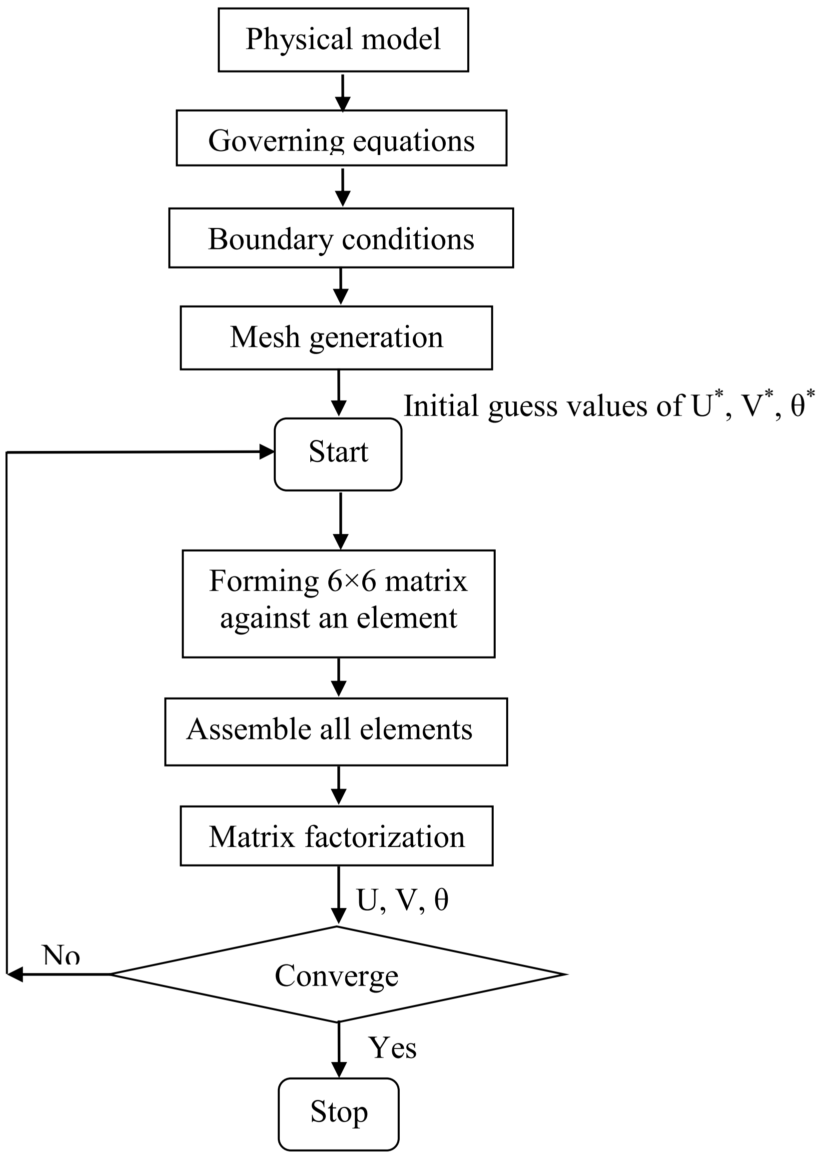

Fig. 2.1 Flow chart of the computational procedure

2.3 Physical Model

The physical model is shown in Fig. 2.2(a) and Fig. 2.2(b), along with the important geometric parameters. In these figures, a heated cylindrical block is made a hole inside the square cavity. The height and the width of the cavity are denoted by H. The length of the cavity perpendicular to its plane is assumed to be long enough; hence the problem is considered two dimensional. Magnetic field of strength B_0 is applied in –x direction and gravity is acted in the vertical direction. The left, upper and right walls of the cavity are kept at cold temperature T_c while the bottom wall and the cylinder are subjected to the heated temperature T_h. In Fig. 2.2(a), the heated cylinder is placed at three different places. In Fig. 2.2(b), the heated cylinder is kept at the midpoint of the cavity and altered the sizes (radius) of cylinder for r = 0.10, 0.20 and 0.30 m. The fluid has been considered as incompressible, Newtonian and the flow was assumed to be laminar. The boundary conditions for velocity have been considered as no-slip on solid boundaries. The thermophysical properties of the fluid have been considered constant with the exception of the density which varies according to the Boussinesq approximation, Gangawane and Bharti (2018).

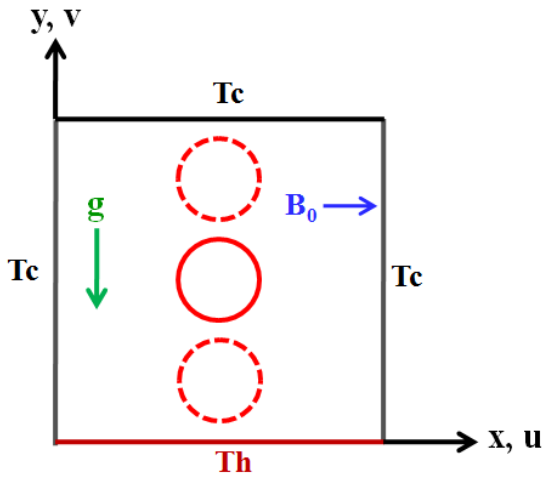

Fig. 2.2(a) Schematic diagram of the physical system for various location of the heated cylinder

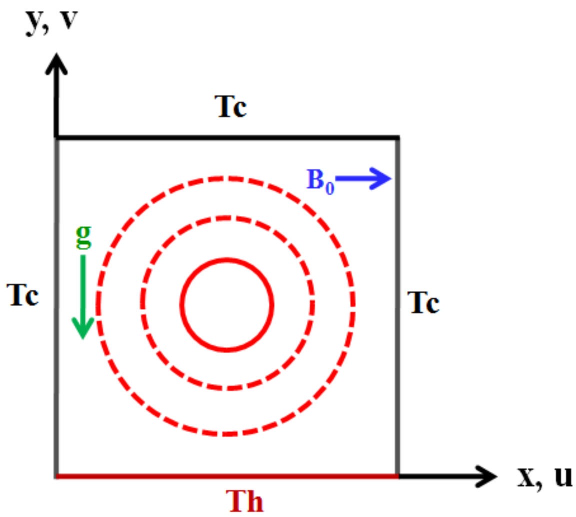

Fig. 2.2(b) Schematic diagram of the physical system for radius variation of the heated cylinder

2.4 Governing equations along with boundary conditions

The electrically conducting fluids are assumed to be Newtonian fluids with constant fluid properties, except for the density in the buoyancy force term. Moreover, the fluid is considered to be laminar, incompressible, steady and two-dimensional. The electrically conducting fluids interact with an external horizontal uniform magnetic field of constant magnetic flux density B_0. Assuming that the flow-induced magnetic field is very small compared to B_0 and considering electrically insulated cavity walls. The electromagnetic force can be reduced to the damping factor $-\sigma B_0^2 v$ [Rahman *et al.* (2009)], where v is the vertical velocity component. Thus the Lorentz force depends only on the velocity component perpendicular to the magnetic field. The governing equations for the two-dimensional steady flow after invoking the Boussinesq approximation and neglecting radiation and viscous dissipation can be expressed as:

Continuity Equation

$$\frac{\partial u}{\partial x}+\frac{\partial v}{\partial y}=0 \qquad (2.1)$$

Momentum Equations

$$\rho\left(u\frac{\partial u}{\partial x}+v\frac{\partial u}{\partial y}\right)=-\frac{\partial p}{\partial x}+\mu\left(\frac{\partial^2 u}{\partial x^2}+\frac{\partial^2 u}{\partial y^2}\right) \qquad (2.2)$$

$$\rho\left(u\frac{\partial v}{\partial x}+v\frac{\partial v}{\partial y}\right)=-\frac{\partial p}{\partial y}+\mu\left(\frac{\partial^2 v}{\partial x^2}+\frac{\partial^2 v}{\partial y^2}\right)+\rho g\beta(T-T_c)-\sigma B_0^2 v \tag{2.3}$$

Energy Equation

$$u\frac{\partial T}{\partial x}+v\frac{\partial T}{\partial y}=\alpha\left(\frac{\partial^2 T}{\partial x^2}+\frac{\partial^2 T}{\partial y^2}\right) \tag{2.4}$$

where *u* and *v* are the velocity components, p is pressure, ρ is the density, μ is the dynamic viscosity, β is the thermal expansion coefficient, σ is the electrical conductivity, B_0 is the magnitude of magnetic field, T is the temperature and α is the thermal diffusivity.

2.4.1 Boundary Conditions

The boundary conditions for the present problem are specified as follows:

At the cylinder:

$$u(x, y) = v(x, y) = 0,\ T(x, y) = T_h \tag{2.5}$$

At the bottom wall:

$$u(x, 0)=0,\ v(x, 0)=0,\ T=T_h\ ;\ \forall\ y=0,\ 0\le x\le H \tag{2.6}$$

At the left wall:

$$u(0, y)=0,\ v(0, y)=0,\ T=T_c;\ \forall\ x=0,\ 0\le y\le H \tag{2.7}$$

At the right wall:

$$u(0, y)=0,\ v(0, y)=0,\ T=T_c;\ \forall\ x=H,\ 0\le y\le H \tag{2.8}$$

At the top wall:

$$u(x, H)=0,\ v(x, H)=0,\ T=T_c;\ \forall\ y=H,\ 0\le x\le H \tag{2.9}$$

where x and y are the distances measured along the horizontal and vertical directions, respectively; u and v are the velocity components in the x- and y-direction, respectively. The height and the width of the cavity are denoted by H. T is denoted temperature; T_h and T_c are denoted heated and cold temperatures respectively.

2.4.2 Non-Dimensional Analysis

Using the following dimensionless parameters, the governing equations (2.1−2.4) can be converted to the non-dimensional forms:

$$X = \frac{x}{H},\ Y = \frac{y}{H},\ U = \frac{uH}{\alpha},\ V = \frac{vH}{\alpha},\ P = \frac{pH^2}{\rho\alpha^2},\ \theta = \frac{T - T_c}{T_h - T_c}$$

where X and Y are the coordinates varying along horizontal and vertical directions, respectively, U and V are the velocity components in the X and Y directions, respectively, θ is the dimensionless temperature and P is the dimensionless pressure. After substituting the above dimensionless variables into the equations (2.1-2.9), we get the following dimensionless equations as:

Continuity Equation

$$\frac{\partial U}{\partial X} + \frac{\partial V}{\partial Y} = 0 \tag{2.10}$$

Momentum Equations

$$U\frac{\partial U}{\partial X} + V\frac{\partial U}{\partial Y} = -\frac{\partial P}{\partial X} + Pr\left(\frac{\partial^2 U}{\partial X^2} + \frac{\partial^2 U}{\partial Y^2}\right) \tag{2.11}$$

$$U\frac{\partial V}{\partial X} + V\frac{\partial V}{\partial Y} = -\frac{\partial P}{\partial Y} + Pr\left(\frac{\partial^2 V}{\partial X^2} + \frac{\partial^2 V}{\partial Y^2}\right) + Ra\,Pr\,\theta - Ha^2\,Pr\,V \tag{2.12}$$

Energy Equation

$$U\frac{\partial \theta}{\partial X} + V\frac{\partial \theta}{\partial Y} = \frac{\partial^2 \theta}{\partial X^2} + \frac{\partial^2 \theta}{\partial Y^2} \tag{2.13}$$

The dimensionless parameters appearing in the equations (2.11) and (2.12) are the Prandtl number Pr, Rayleigh number Ra, and Hartmann number Ha. They are respectively defined as follows:

$$Pr = \frac{\mu}{\rho\alpha},\ Ra = \frac{g\beta(T_h - T_c)H^3}{\alpha v},\ Ha = B_0 H\sqrt{\frac{\sigma}{\mu}} \tag{2.14}$$

2.4.3 Non-Dimensional Boundary Conditions

The non- dimensional boundary conditions under consideration can be written as:

At the cylinder:

$$U = 0,\ V = 0,\ \Theta = 1 \tag{2.15}$$

At the bottom wall:

$$U = 0,\ V = 0,\ \theta = 1;\ \forall Y = 0 \text{ and } 0 \le X \le 1 \tag{2.16}$$

At the left wall:

$$U = 0,\ V = 0,\ \theta = 0;\ \forall X = 0 \text{ and } 0 \le Y \le 1 \tag{2.17}$$

At the right wall:

$$U = 0,\ V = 0,\ \theta = 0;\ \forall X = 1 \text{ and } 0 \le Y \le 1 \tag{2.18}$$

At the top wall:

$$U = 0,\ V = 0,\ \theta = 0;\ \forall Y = 1 \text{ and } 0 \le X \le 1 \tag{2.19}$$

where X and Y are dimensionless coordinates varying along horizontal and vertical directions, respectively; U and V are dimensionless velocity components in X and Y directions, respectively; Θ is the dimensionless temperature. Once the velocity and temperature fields were obtained, the local and surface-averaged Nusselt numbers were calculated as follows:

$$Nu = \left.\frac{\partial\theta}{\partial n}\right|_{\text{cylinder's wall}},\quad Nu_{av} = \frac{1}{S}\int_0^S Nu\, dS \tag{2.20}$$

where n is the direction normal to the cylinder's wall and S is the surface area of the cylinder.

2.5 Numerical Analysis

The governing equations along with the boundary conditions have been solved numerically, employing Galerkin weighted residual finite element techniques, Zienkiewicz and Taylor (1989). The solution flow-charts and detailed computational processes have not been discussed in this research because the whole numerical analysis system has retained in built-in process of Comsol Multi-physics.

2.6 Grid Size Sensitivity Test

A grid independence study was executed to make sure the correctness of the numerical results for the square cavity at the representative value of Ra = 10^5, Ha = 50, Pr = 0.71, CP at (0.50, 0.50) and size of the cylinder, r = 0.20 m. It has been observed in Table 2.1 and Fig. 2.4 that the average Nusselt number (Nu_{av}) for 6614 elements has shown little difference with the results obtained for the other higher elements. So, the element 6820 has chosen for further calculations of both cases: position variation of cylinder and size (radius) variation of cylinder.

Table 2.1: Grid Sensitivity Check at Ra = 10^5, Ha = 50, Pr = 0.71 and r = 0.20 m, CP at (0.50, 0.50).

Elements	1666	2458	3496	4396	5436	6614	6820	9568
Nu_{av}	3.646	3.962	4.149	4.309	4.451	4.513	4.519	4.545
Time(s)	9	14	21	28	40	51	63	78

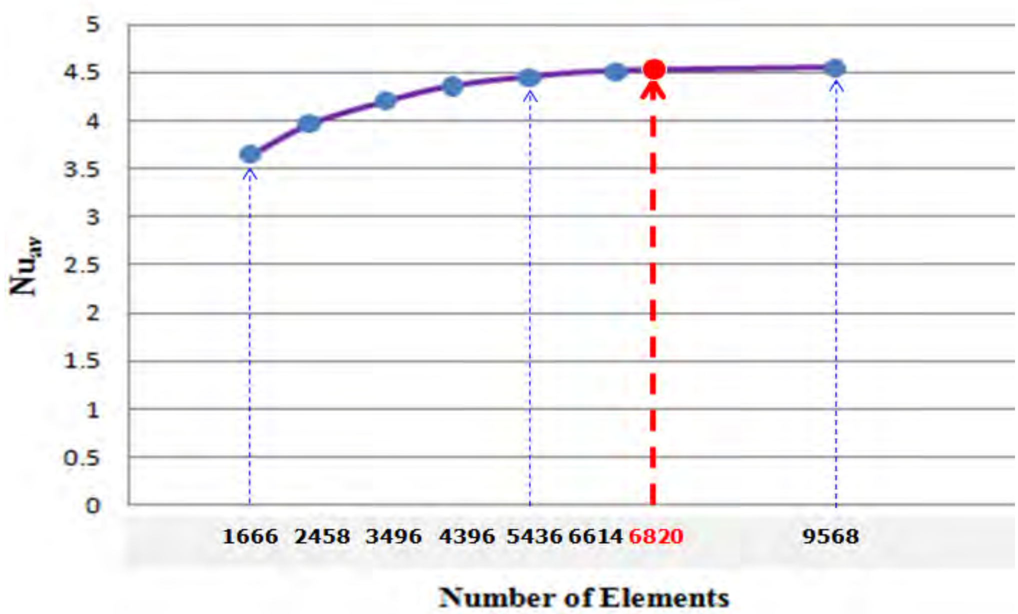

Fig. 2.3 Grid independency study for different elements, where Ra = 10^5, Ha = 50, Pr = 0.71 and r = 0.20 m.

2.7 Validation of the Numerical Scheme

In order to verify the accuracy of the numerical results and the validity of the mathematical model obtained throughout the present study, comparisons with the previously published results are essential. But due to the lack of availability of experimental data on the particular problems along with its associated boundary conditions investigated in this study, validation of the predictions could not be done against experiment. However, the outcome of the present numerical code is benchmarked against the numerical result of Jani *et al.* (2013) which was reported for

Magnetohydrodynamic free convection in a square cavity heated from below and cooled from other walls. The streamlines and isotherms for Pr = 0.71, Ra = 10^6, and different Hartmann numbers have been presented in the Fig. 2.4 (a-b) that is a good agreement with Jani *et al.* (2013). As a result the validation boosts the confidence in the numerical code to carry on with the above stated objective of the current investigation.

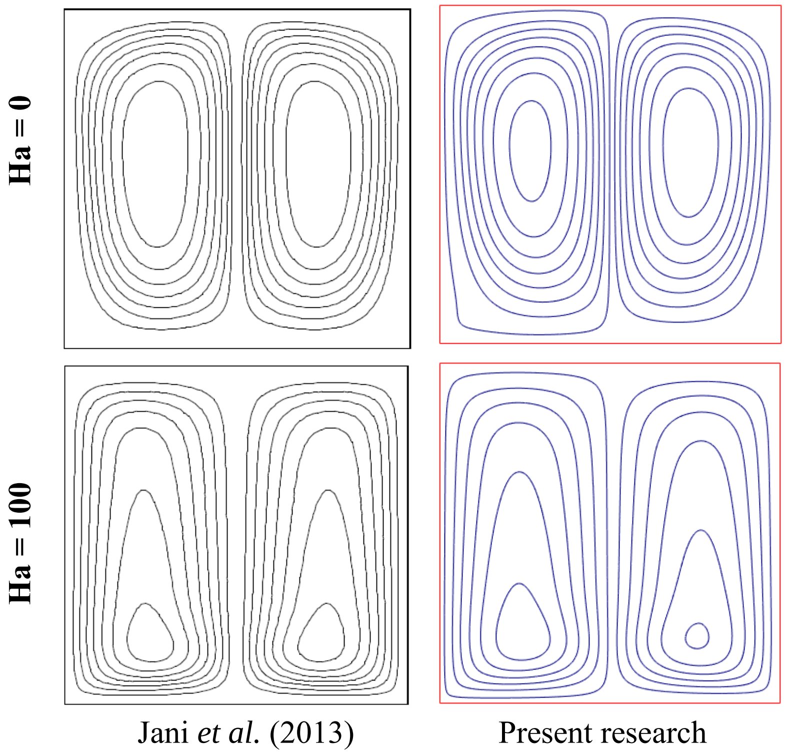

Fig. 2.4(a) Comparison of streamlines between present research and Jani *et al*. (2013) where Ra = 10^6, Pr = 0.71 for different Ha.

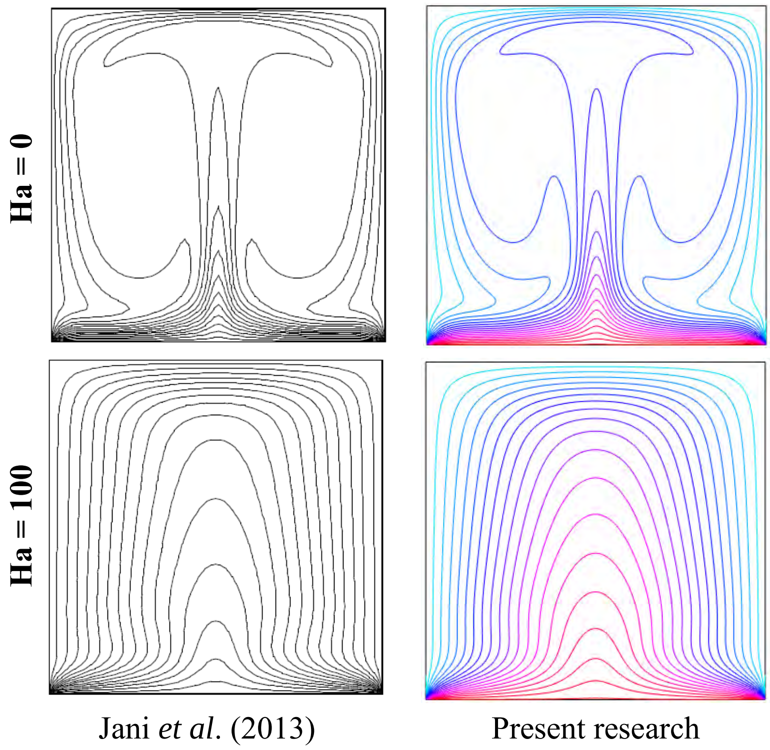

Fig. 2.4(b) Comparison of isothermal lines between present research and Jani *et al*. (2013), where Ra = 10^6, Pr = 0.71 for different Ha.

CHAPTER 3

RESULTS AND DISCUSSIONS

As stated earlier, the overall objective of the current chapter is to explore the effects of cylinder location and size on MHD natural convection flow in a square cavity with the help of finite-element method. Numerical results have been depicted in order to determine the effects of the considered parameters. The relevant parameters in the present study are buoyancy parameter, Rayleigh number ($10^4 \le \mathrm{Ra} \le 5\times10^6$), magnetic field parameter, Hartmann number ($0 \le \mathrm{Ha} \le 50$) and the thermal diffusivity parameter, Prandtl number ($0.71 \le \mathrm{Pr} \le 10$). The physical parameter for the system is the radius of the heated cylinder (r). In this research, two cases have been performed: (case I) location of the heated cylinder is taken to the different positions at (0.50, 0.25), (0.50, 0.50) and (0.50, 0.75) in the square cavity where the size (radius) is fixed for r = 0.20 m and (case II) size (radius) of the heated cylinder is altered from 0.10 m to 0.30 m where the cylinder has been kept at the centre of the square cavity at (0.50, 0.50). The results have been presented in terms of streamlines, isotherms, average velocity magnitude, average Nusselt number, average fluid temperature and related graphs and charts.

3.1 Case I (Variation of cylinder’s position)

In this case, the heated cylinder’s position (CP) is considered at various places in the square cavity. It has supposed to take only three locations of cylinder out of multiple positions. The positions have been considered at (0.50, 0.25), (0.50, 0.50) and (0.50, 0.75) of the square cavity. Effects of Rayleigh number (Ra), Hartmann number (Ha) and Prandtl number (Pr) have discussed in this case.

3.1.1 Effects of Rayleigh number

The influences of the different positions of the heated cylinder inside the square cavity have been performed in terms of different non-dimensional numbers.

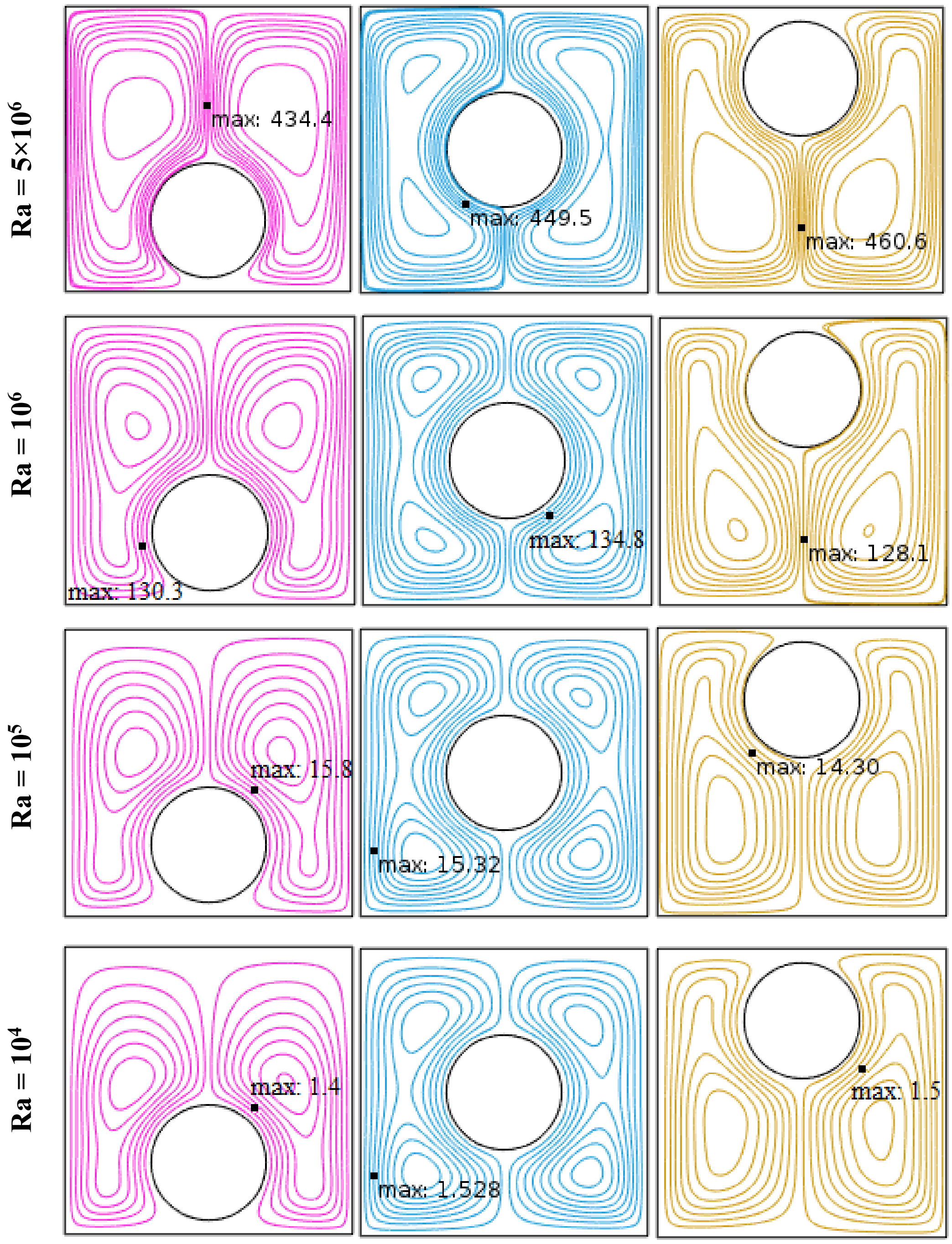

(a) (0.50, 0.25) **(b) (0.50, 0.50)** **(c) (0.50, 0.75)**

Fig. 3.1 (a-c) Streamlines for different Ra and different positions of cylinder, where Pr = 0.71, r = 0.20 m and Ha = 50.

The effects of Rayleigh number (Ra = 10^4, 10^5, 10^6, 5×10^6) on streamlines for the present configuration for Ha = 50 and Pr = 0.71 has been presented in figure 3.1(a - c) where the cylinder's positions (CP) are at (0.50, 0.25), (0.50, 0.50) and (0.50, 0.75) of the cavity and the size (radius) r = 0.20 m.

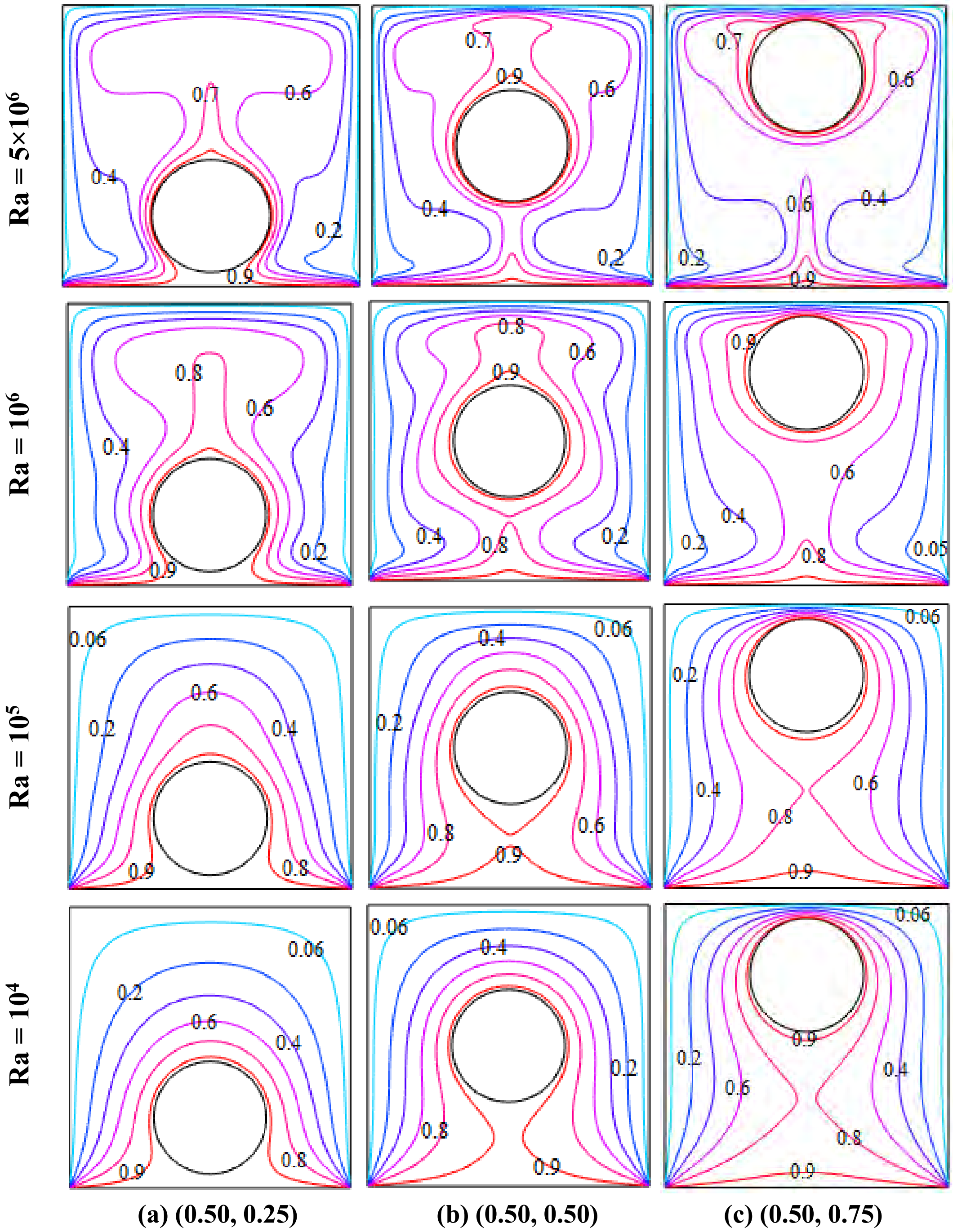

Fig. 3.2 (a-c) Isothermal lines for different Ra and different positions of cylinder, where Pr = 0.71, r = 0.20 m and Ha = 50.

It is observed that the velocity magnitude is increasing quickly with the increase of Rayleigh number from Ra = 10^4 to 5×10^6 for three different positions of the cavity. The maximum vorticity is 460.6 (m/s) at (0.50, 0.20) for Ra = 5×10^6, where CP at (0.50, 0.75), Ha = 50, Pr = 0.71 and size (radius) of the cylinder, r = 0.20 m.

The isotherms for different Rayleigh numbers with three different positions have been exhibited in Fig. 3.2 (a-c). When CP at (0.50, 0.25), the heated isothermal lines have been changed their directions gradually for different Ra and no isotherm lines have found between the heated cylinder and the bottom wall. When CP at (0.50, 0.75), it has been observed that most of the isotherms have congested between the top wall and the heated cylinder. Some isothermal lines have been formed blooms above the cylinder for CP at (0.50, 0.50) and Ra = 5×10^6.

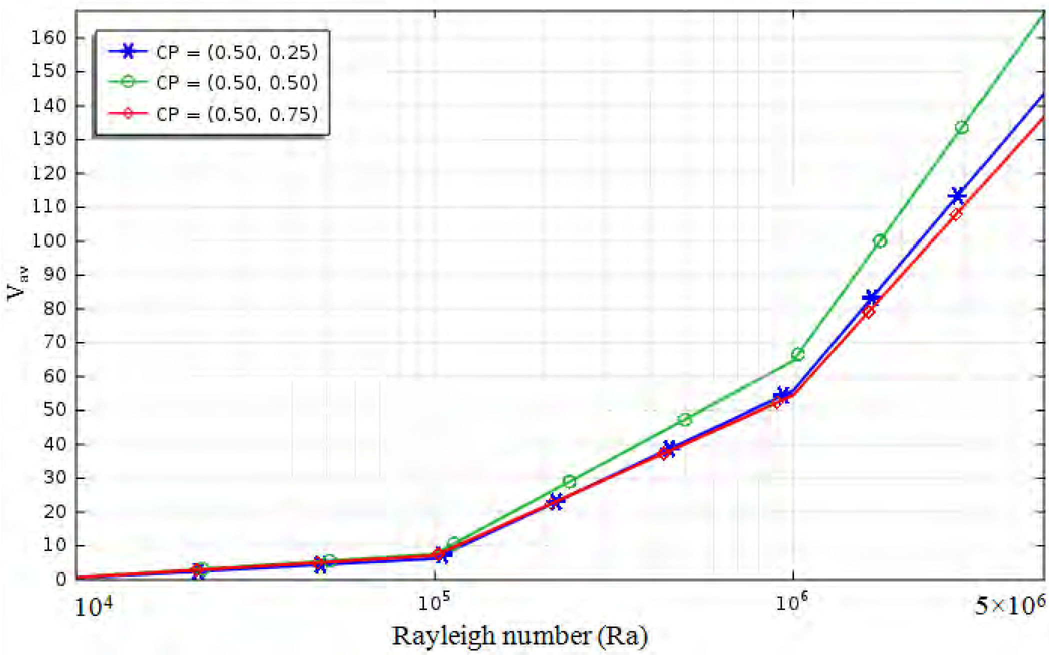

Fig. 3.3 Effect of Rayleigh number (Ra) on average velocity magnitude (V_{av}) for different positions of the cylinder, where Pr = 0.71, Ha = 50 and r = 0.20 m.

The effect of Rayleigh number (Ra) on average velocity magnitude (V_{av}) for different CP, where Pr = 0.71, Ha = 50 and r = 0.20 m has revealed in Fig. 3.3. It has been viewed that the V_{av} has increased slowly for Ra = 10^4 to 10^5 and then raising rapidly for Ra = 10^5 to 5×10^6. Besides, V_{av} is always greater for Ra = 10^5 to 5×10^6, CP at (0.50, 0.50) compare to the other positions of the cylinder.

Fig. 3.4 displays the average Nusselt number (Nu_{av}) along the heated cylinder for different positions (0.50, 0.25), (0.50, 0.50) and (0.50, 0.75) of the cylinder. For all of the locations of cylinder, the Nu_{av} has been decreased slowly when Ra = 10^4 to 10^5 and then increased when Ra = 10^5 to 5×10^6. It has been viewed that the Nu_{av} has increased with the location variation of heated cylinder from heated bottom wall to the cold top wall of the cavity.

Fig. 3.5 shows the average fluid temperature (Θ_{av}) in the cavity for different locations of the heated cylinder. When CP at (0.50, 0.25), the Θ_{av} is increased for Ra = 10^4 to 10^6 and then unchanged for Ra = 10^6 to 5×10^6. On the other hand, the Θ_{av} decreases for Ra = 10^5 to 5×10^6.

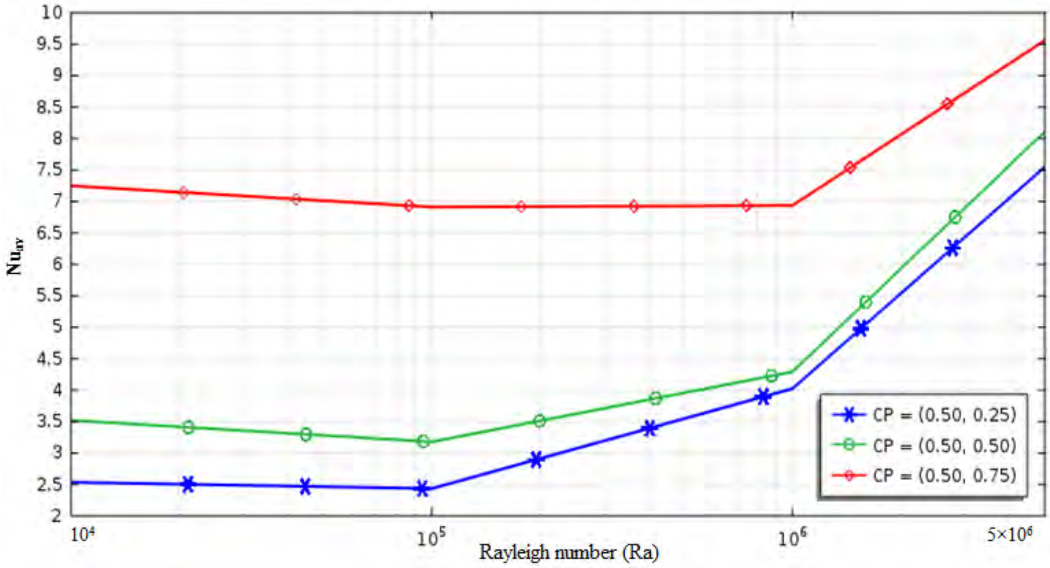

Fig. 3.4 Effect of Rayleigh number (Ra) on average Nusselt number (Nu_{av}) for different positions of the cylinder, where Pr = 0.71, Ha = 50 and r = 0.20 m.

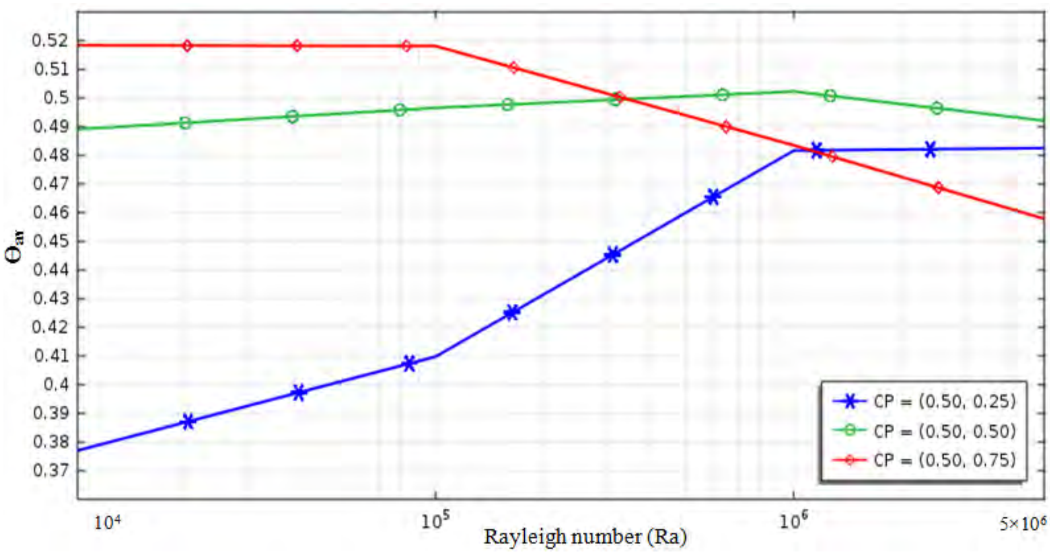

Fig. 3.5 Effect of Rayleigh number (Ra) on average fluid temperature (Θ_{av}) for different positions of the cylinder, where Pr = 0.71, Ha = 50 and r = 0.20 m.

3.1.2 Effects of Hartmann number

A numerical analysis has been performed in this research to investigate the effects of Hartmann number (Ha) with different positions of the heated cylinder in the cavity while Ra and Pr are fixed at 10^4 and 0.71, respectively. The investigated results are presented in terms of streamlines, isotherms, average velocity magnitude (V_{av}), average Nusselt number (Nu_{av}) and average fluid temperature (Θ_{av}). Fig. 3.6 (a-c) displays the streamlines for different Hartmann numbers with three different positions (0.50, 0.25), (0.5, 0.50), and (0.50, 0.75) of the cylinder. The strength of velocity magnitude is decreased with the increase of Hartmann number for different locations of the heated cylinder in the cavity. In the absence of magnetic effect (Ha = 0), the maximum vorticity (11.05 m/s) is found at (0.90, 0.36) when CP at (0.50, 0.75), size (radius) of the cylinder, r = 0.20 m, Ra = 10^4 and Pr = 0.71.

Fig. 3.7 (a-c) exhibit the isotherms for different Hartmann number with three different positions at (0.50, 0.25), (0.50, 0.50), and (0.50, 0.75) of cylinder in the cavity. When CP at (0.50, 0.25), the isotherms are altered their directions very mildly with the change of Ha from 0 to 50. When CP at (0.50, 0.75), a small number of heated isothermal lines are surrounded along the heated cylinder. It has been viewed that a number of isothermal contours have concentrated between top wall and the heated cylinder when CP at (0.50, 0.75).

Fig. 3.8 explores the outcome of Hartmann numbers on V_{av} for different CP, where Pr = 0.71, Ra = 10^4 and r = 0.20 m. The average velocity magnitude (V_{av}) declines with the increase of Hartmann number (Ha) from 0 to 50. It is clear that the V_{av} increases with the CP variations from bottom wall to top wall of the cavity for Ha = 0 to 22.

Fig. 3.9 displays the effect of Hartmann number on Nu_{av} for different CP, where Pr = 0.71, Ra = 10^4 and r = 0.20 m. When CP at (0.50, 0.25), the Nu_{av} is approximately same (2.6) for Ha = 0 to 50. When CP at (0.50, 0.50) and (0.50, 0.75), the Nu_{av} is rising very slowly with the increase of Hartmann number from 0 to 50.

Effect of Hartmann number on average fluid temperature (Θ_{av}) in the cavity for different positions of the cylinder is examined in the Fig. 3.10. When CP at (0.50, 0.25), the Θ_{av} declines slowly for Ha = 0 to 50. On the other hand, for CP at (0.50, 0.75), the Θ_{av} increases very slowly for Ha = 0 to 50 and mentionable change of Θ_{av} is not found for CP at (0.50, 0.50).

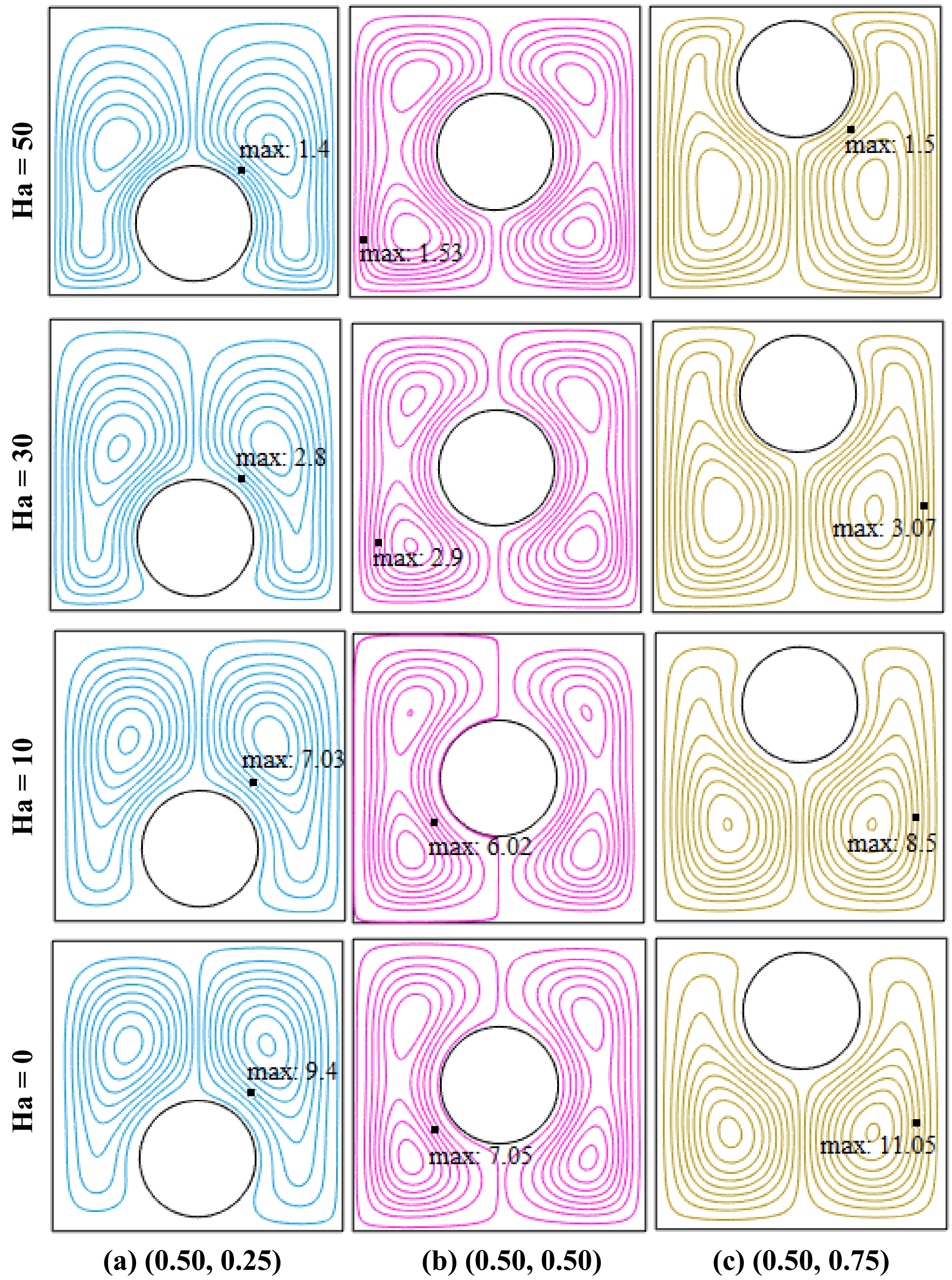

Fig. 3.6 (a-c) Streamlines for different Ha and different positions of cylinder, where Pr = 0.71, r = 0.20 m and Ra = 10^4.

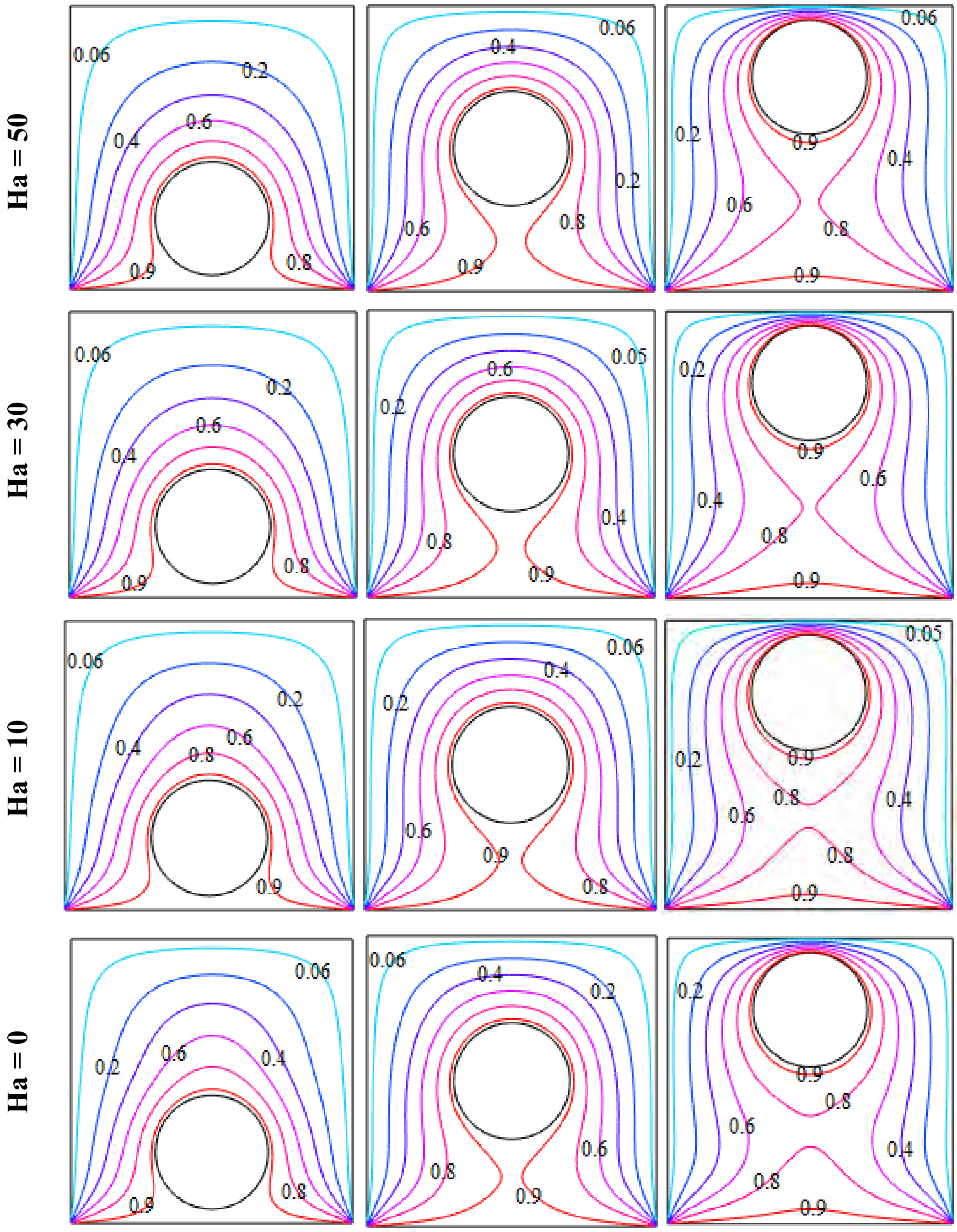

(a) (0.50, 0.25) **(b) (0.50, 0.50)** **(c) (0.50, 0.75)**

Fig. 3.7 (a-c) Isothermal lines for different Ha and different positions of cylinder, where Pr = 0.71, r = 0.20 m and Ra = 10^4.

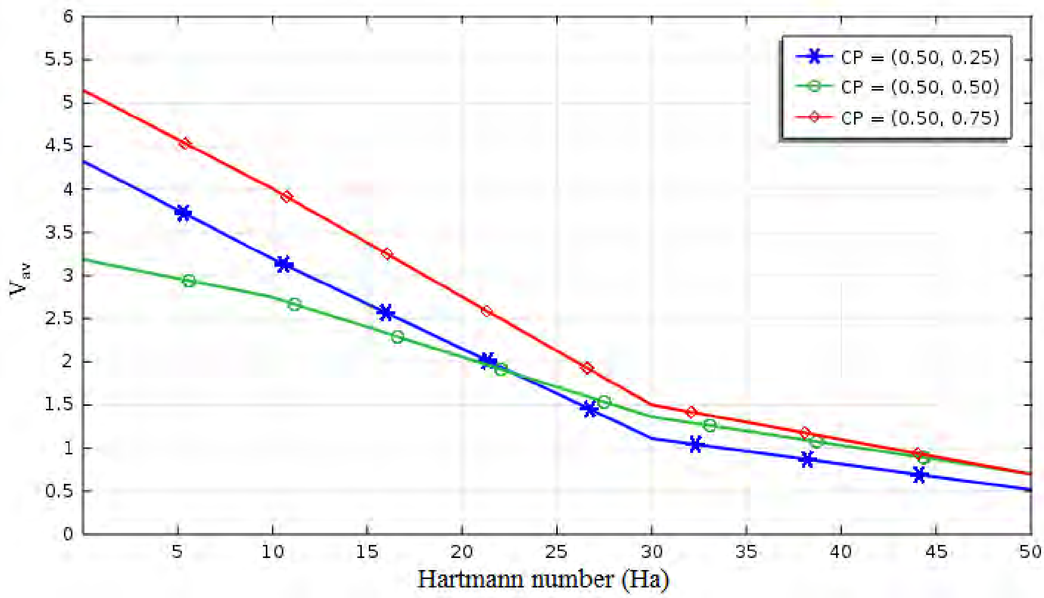

Fig. 3.8 Effect of Hartmann number (Ha) on average velocity magnitude (V_{av}) for different positions of the cylinder, where Pr = 0.71, Ra = 10^4 and r = 0.20 m.

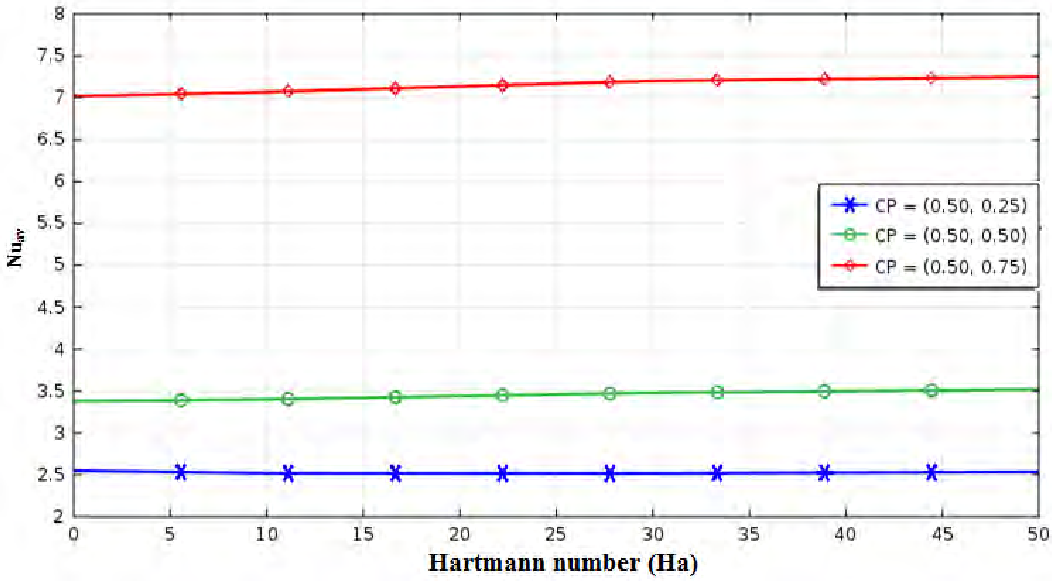

Fig. 3.9 Effect of Hartmann number (Ha) on average Nusselt number (Nu_{av}) for different positions of the cylinder, where Pr = 0.71, Ra = 10^4 and r = 0.20 m.

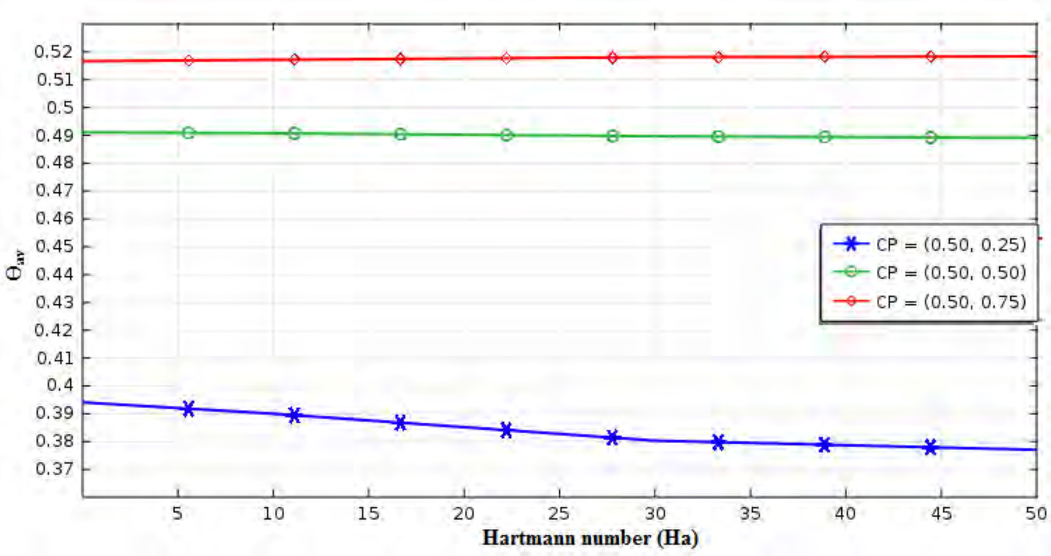

Fig. 3.10 Effect of Hartmann number (Ha) on average fluid temperature (Θ_{av}) for different positions of the cylinder, where Pr = 0.71, Ra = 10^4 and r = 0.20 m.

3.1.3 Effects of Prandtl number

The effects of Prandtl number (Pr) on the velocity profile and thermal field in terms of streamlines and isotherms are presented in figure 3.11 and 3.12, respectively. Fig. 3.11 (a-c) displays the streamlines for different CP and different Prandtl numbers (Pr) from 0.71 to 10. The strength of the velocity magnitude increases with the increase of Pr from 0.71 to 10 and different positions of the heated cylinder. The maximum vorticity (3.29 m/s) displays at (0.37, 0.67) for Pr = 10 when CP at (0.50, 0.50), Ha = 50, Ra = 10^4 and r = 0.20 m.

Fig. 3.12 (a-c) exhibits the isothermal lines for different locations of the heated cylinder with Pr = 0.71 to 10, r = 0.20 m, Ha = 50, Ra = 10^4. Fig. 3.12(a) exhibits that the isothermal lines are squeezed gradually above the heated cylinder for large Pr number (Pr = 5 and 10) When the CP at (0.50, 0.75), lots of isothermal lines have been clustered between top wall and the heated cylinder.

Fig. 3.13 displays the outcome of Prandtl number (Pr) on average velocity magnitude (V_{av}) for different CP, where Ha = 50, Ra = 10^4 and r = 0.20 m. The highest velocity magnitude (1.13 m/s) in the cavity is found when CP at (0.50, 0.50), Pr = 10 and r = 0.20 m. Besides, V_{av} is altering upwardly always for position variation of the heated cylinder from bottom wall to top wall of the cavity.

Fig. 3.14 presents the effect of Prandtl number on average Nusselt number (Nu_{av}) for different CP, where Ha = 50, Ra = 10^4 and r = 0.20 m. When CP at (0.50, 0.25), the Nu_{av} decreases for Pr = 0.71 to 5 and then Nu_{av} increases slowly for Pr = 5 to 10. When CP at (0.50, 0.50) and (0.50, 0.75), the Nu_{av} decreases very slowly with the increase of Prandtl number from 0.71 to 10.

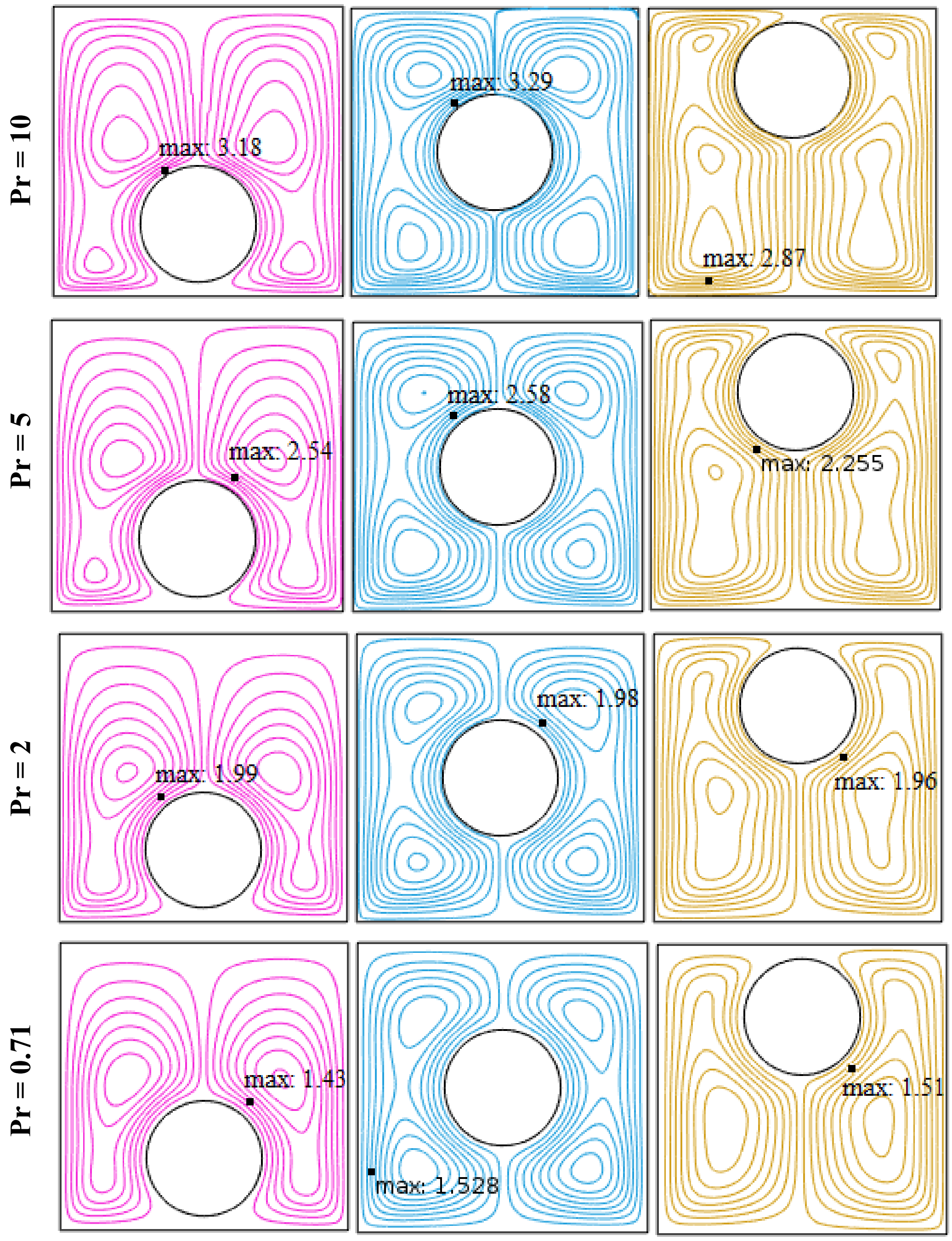

(a) (0.50, 0.25) **(b) (0.50, 0.50)** **(c) (0.50, 0.75)**

Fig. 3.11 (a-c) Streamlines for different Pr and different positions of cylinder, where Ha = 50, Ra = 10^4 and r = 0.20 m.

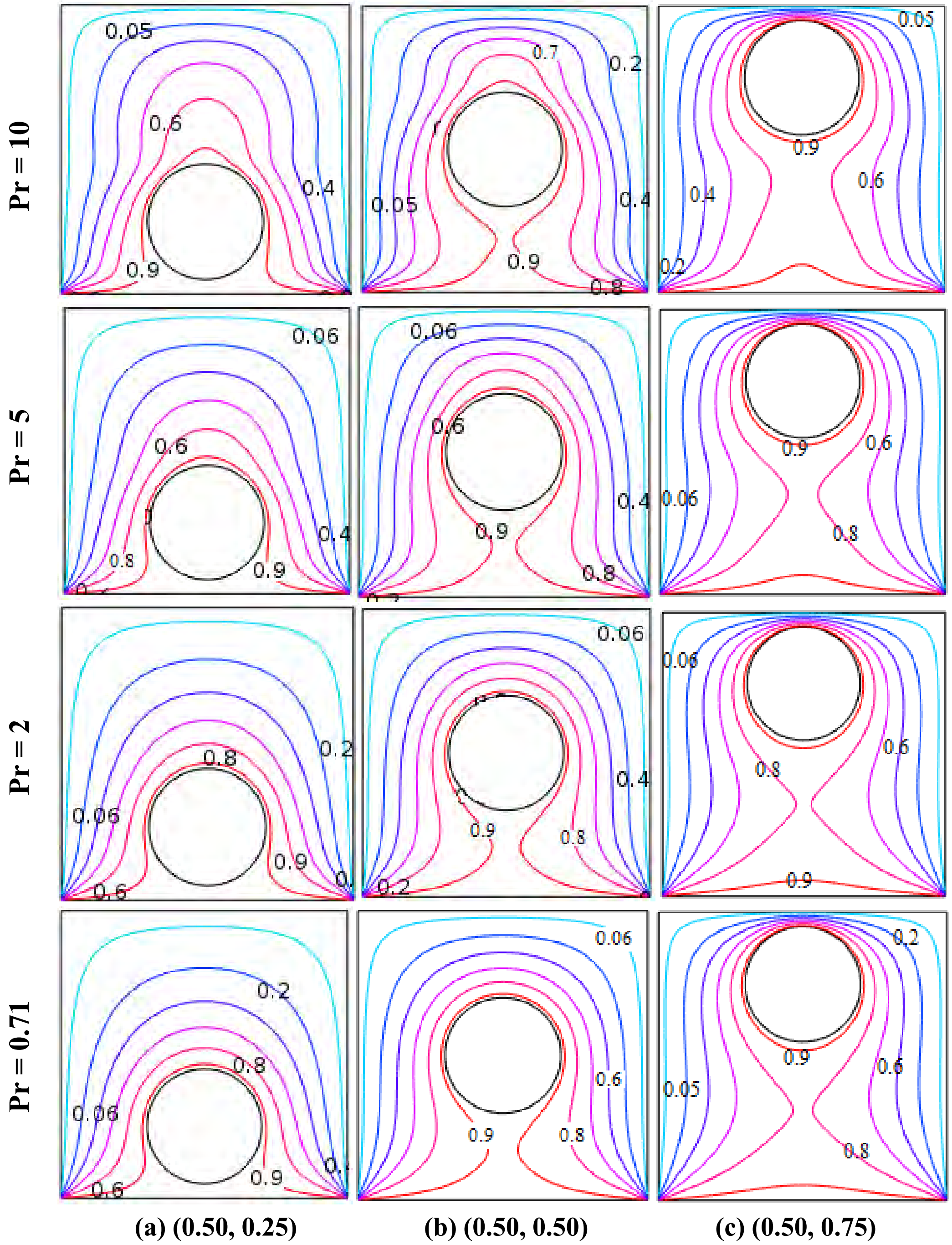

Fig. 3.12 (a-c) Isothermal lines for different Pr and different positions of cylinder, where Ha = 50, Ra = 10^4 and r = 0.20 m.

Effect of Prandtl numbers on average fluid temperature (Θ_{av}) in the cavity for different positions of the cylinder has exhibited in Fig. 3.15. It is viewed that, for all locations of the heated cylinder, the Θ_{av} increases with the increase of Pr from 0.71 to 10. Besides, Θ_{av} varies from 0.377 to 0.530 for three positions of the heated cylinder.

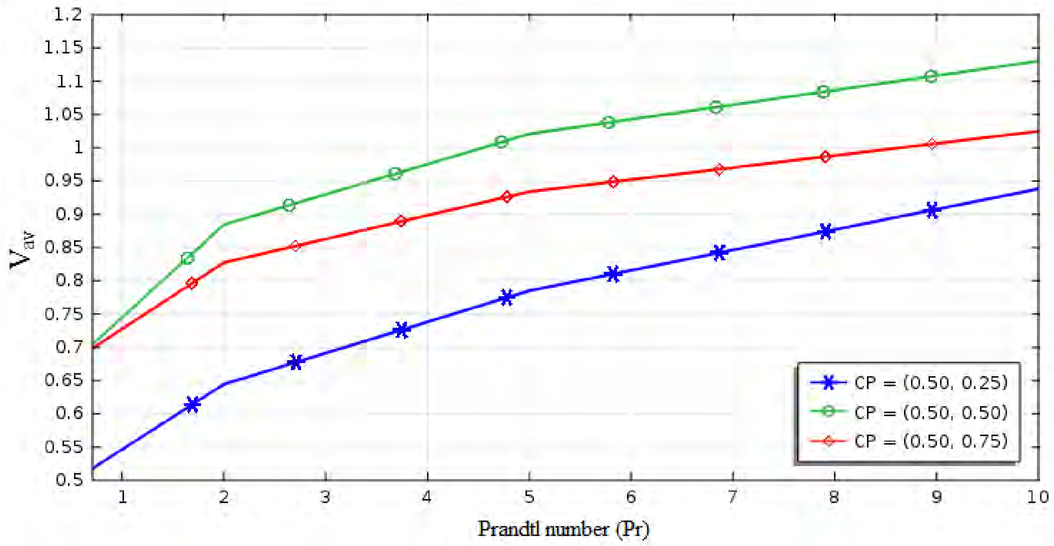

Fig. 3.13 Effect of Prandtl number (Pr) on average velocity magnitude (V_{av}) for different positions of the cylinder, where Ha = 50, Ra = 10^4 and r = 0.20 m.

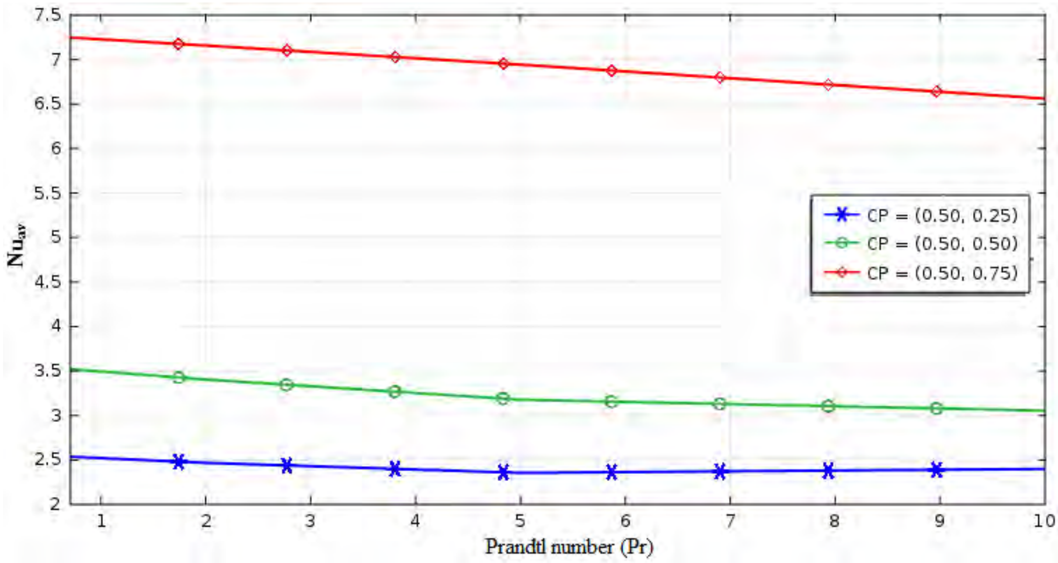

Fig. 3.14 Effect of Prandtl number on average Nusselt number (Nu_{av}) for different positions of the cylinder, where Ha = 50, Ra = 10^4 and r = 0.20 m.

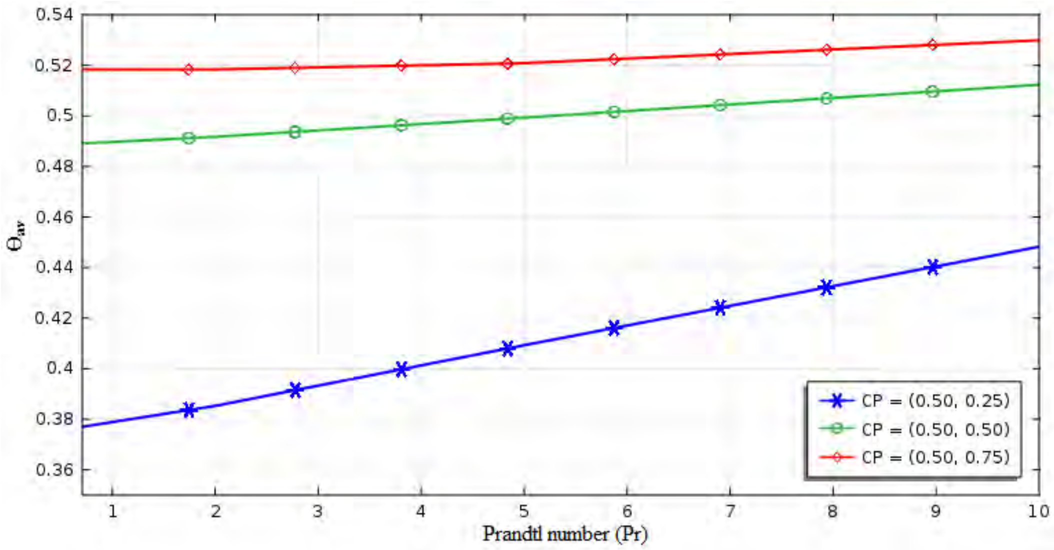

Fig. 3.15 Effect of Prandtl number (Pr) on average fluid temperature (Θ_{av}) for different positions of the cylinder, where Ha = 50, Ra = 10^4 and r = 0.20 m.

3.2 Case II (Variation of cylinder size)

In this case, the size of the heated cylinder has been altered from r = 0.10 to 0.30 m and the position of the cylinder has been kept at the centre (0.50, 0.50) of the cavity. It is supposed to take only three sizes of the cylinder whose radii are r = 0.10, 0.20 and 0.30 m, respectively. Effects of Rayleigh number (Ra), Hartmann number (Ha) and Prandtl number (Pr) have been discussed in this case.

3.2.1 Effects of Rayleigh number

The influences of different sizes of the heated cylinder at the center of the square cavity have been performed in terms of different non-dimensional numbers. The effects of Rayleigh number (Ra = 10^4, 10^5, 10^6, 5×10^6) on streamlines for the present configuration for Ha = 50 and Pr = 0.71 is exhibited in fig. 3.16 (a-c). It is observed in the Fig. 3.16 (a-c) that the strength of the velocity magnitude increases with the increase of Rayleigh number (Ra) from Ra = 10^4, 10^5, 10^6, 5×10^6 for all sizes of the heated cylinder in the cavity. The biggest vorticity (466.4 m/s) of the streamlines is viewed at (0.50, 0.25) in the cavity where Ra = 5×10^6, r = 0.10 m, Ha = 50 and Pr = 0.71. From the above discussion it can be proclaimed when absence of any obstacle like cylinder, the fluid velocity is affected more in the cavity.

Fig. 3.17 (a-c) displays the isothermal lines for different Rayleigh numbers with three sizes (r = 0.10, 0.20, 0.30 m) of the heated cylinder in the cavity. When r = 0.10 m, some heated isotherms are found between cylinder and heated bottom wall. A few number of heated isotherms are congested around the heated cylinder when Ra = 10^6 to 5×10^6, r = 0.20 to r = 0.30 m. In addition, some buds are viewed above the heated cylinder when Ra = 10^6 and 5×10^6.

Effect of Rayleigh numbers on average velocity magnitude (V_{av}) in the cavity for different sizes of the cylinder is shown in Fig. 3.18. For all sizes of the heated cylinder, the V_{av} increases with the increase of Rayleigh number (Ra = 10^4 to 5×10^6). Also for Ra = 10^4 to 10^5, the V_{av} increases very slowly for different sizes of heated cylinders. The greatest velocity magnitude (184 m/s) is viewed when Ra = 5×10^6, size, r = 0.30 m, Pr = 0.71, Ha = 50 and CP at (0.50, 0.50).

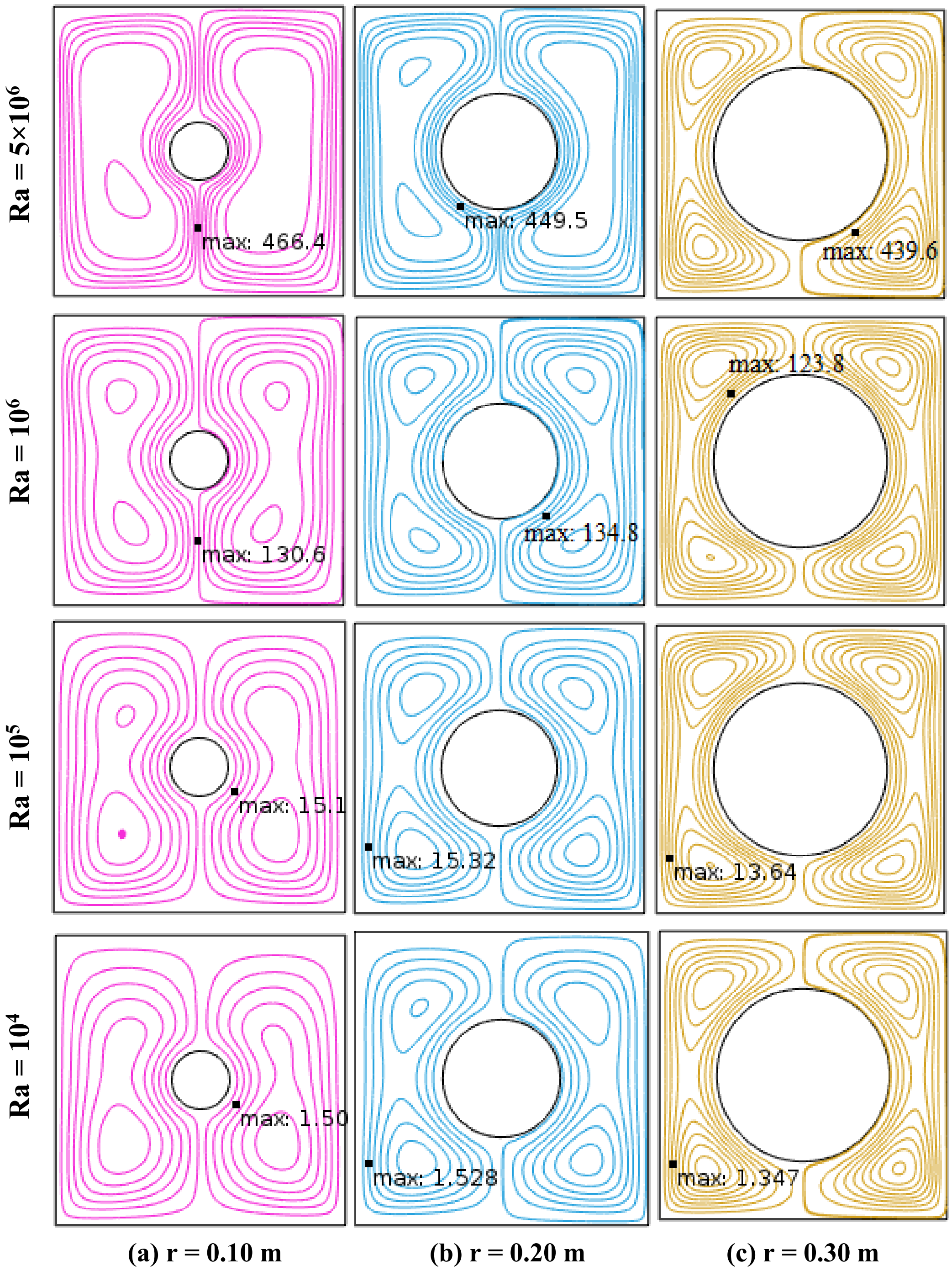

Fig. 3.16 (a-c) Streamlines for different Ra and different sizes of cylinder, where Pr = 0.71, Ha = 50 and CP at (0.50, 0.50).

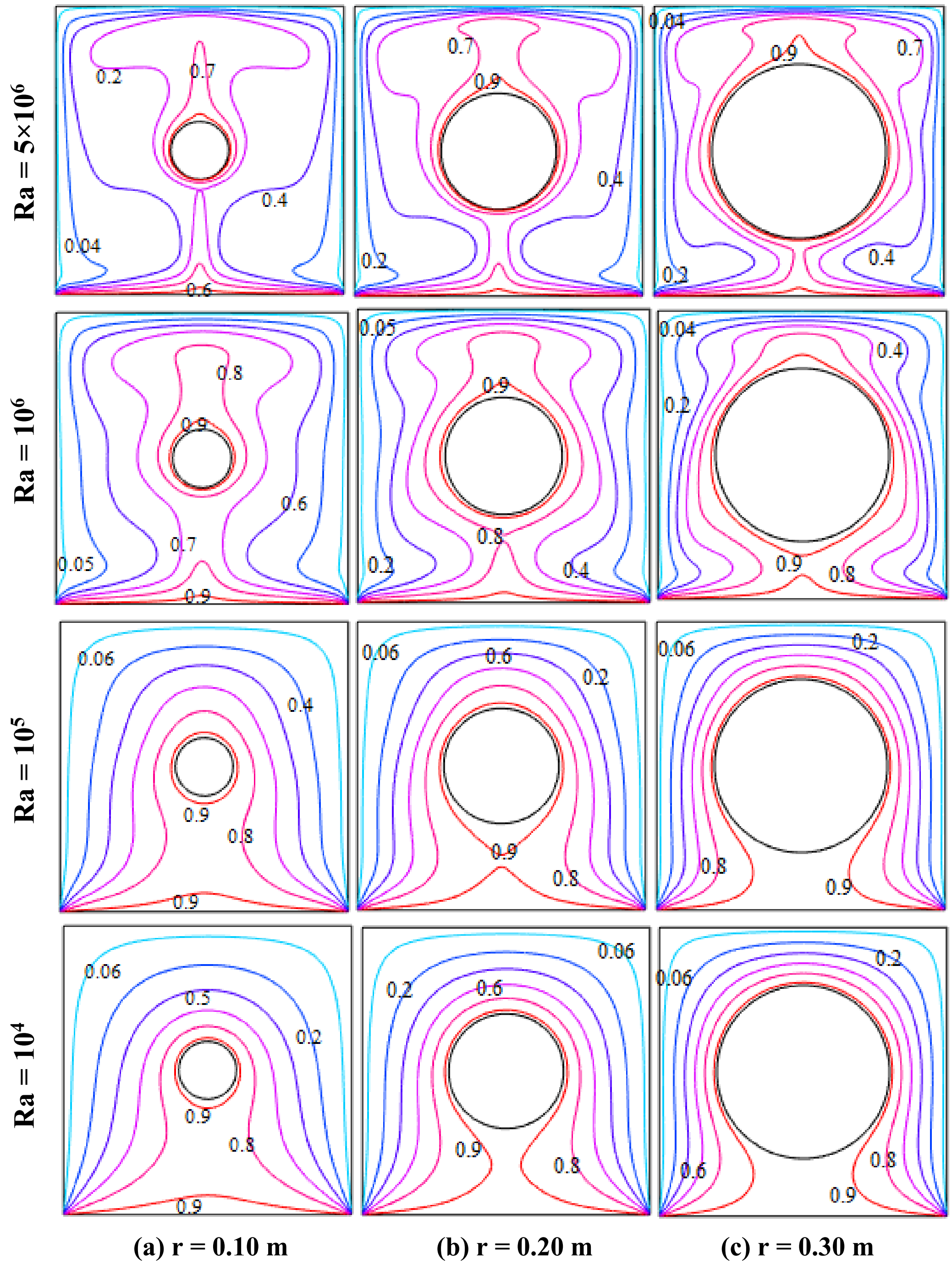

Fig. 3.17 (a-c) Isothermal lines for different Ra and different sizes of cylinder, where Pr = 0.71, Ha = 50 and CP at (0.50, 0.50).

Fig. 3.19 displays the effect of Rayleigh number (Ra) on Nu_{av} for different sizes of heated cylinder, where Ha = 50, Pr = 0.71 and CP at (0.50, 0.50). The Nu_{av} declines incredibly when Ra = 10^4 to 10^5 for different sizes of the cylinder and Nu_{av} improves particularly for Ra = 10^6 to 5×10^6 quickly because the strong buoyancy force causes higher heat transfer rate.

Fig. 3.20 shows the average fluid temperature (Θ_{av}) in the cavity for different sizes of the heated cylinder, where Pr = 0.71, Ha = 50, CP at (0.50, 0.50) and Rayleigh number Ra = 10^4 to 5×10^6. For all sizes of the cylinders, the Θ_{av} improves gradually for Ra = 10^4 to 10^6 and then decreases for Ra = 10^6 to 5×10^6. Moreover, the average fluid temperature (Θ_{av}) improves when the size of the heated cylinder is upturned from r = 0.10 to r = 0.30 m.

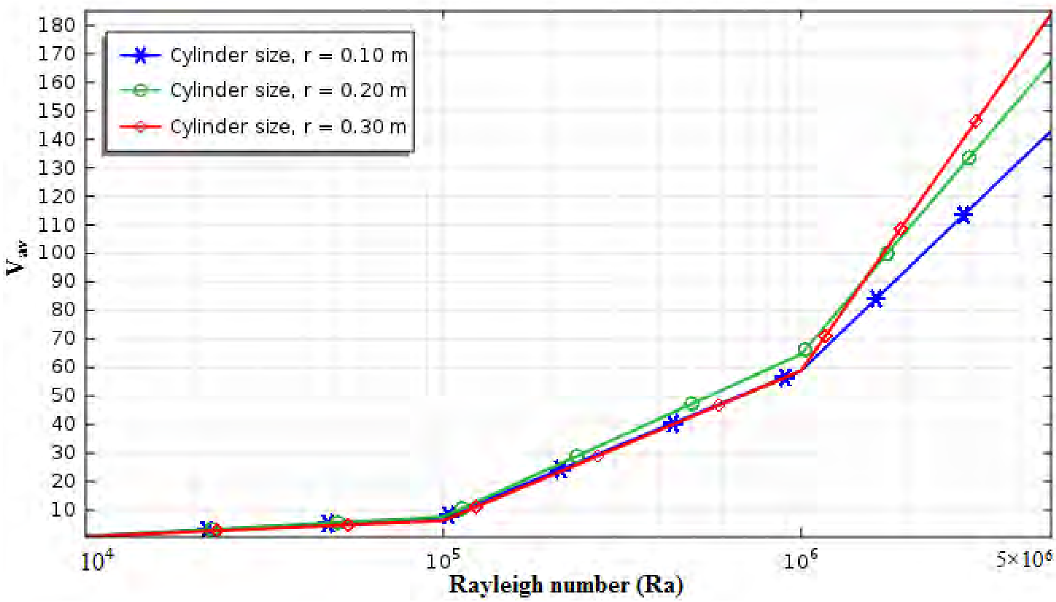

Fig. 3.18 Effect of Rayleigh number (Ra) on average velocity magnitude (V_{av}) for different sizes of the cylinder, where Pr = 0.71, Ha = 50 and CP at (0.50, 0.50).

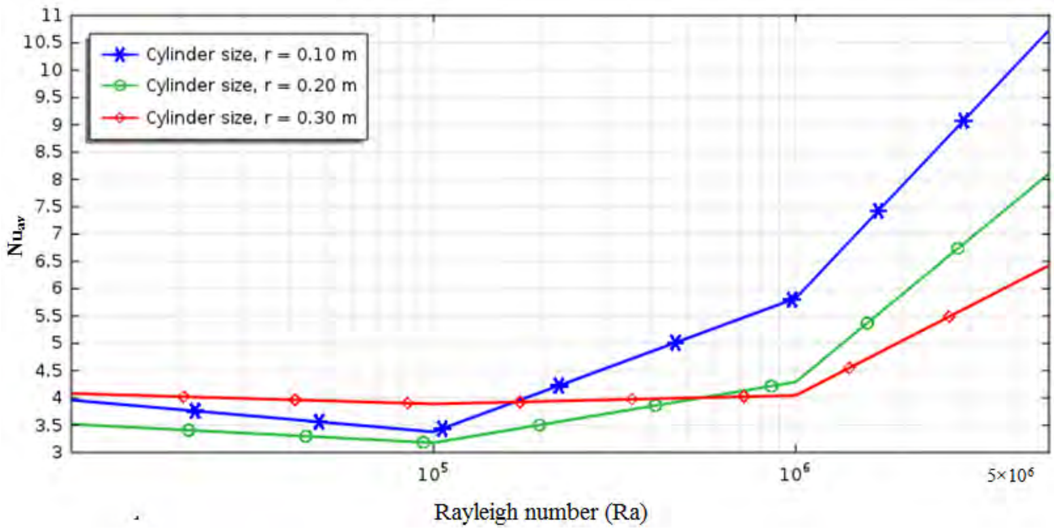

Fig. 3.19 Effect of Rayleigh number (Ra) on average Nusselt number (Nu_{av}) for different sizes of the cylinder, where Pr = 0.71, Ha = 50 and CP at (0.50, 0.50).

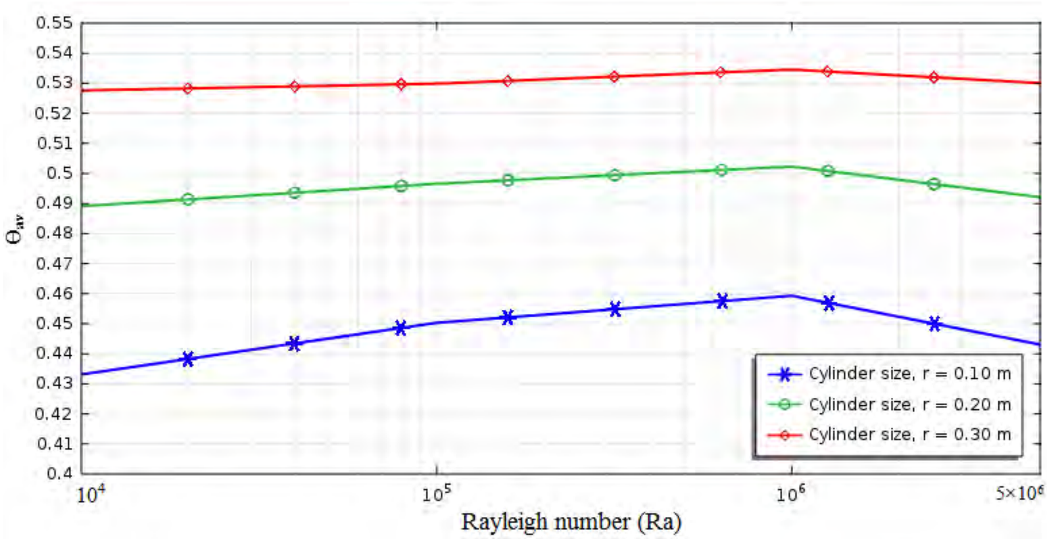

Fig. 3.20 Effect of Rayleigh number (Ra) on average fluid temperature (Θ_{av}) for different sizes of the cylinder, where Pr = 0.71, Ha = 50 and CP at (0.50, 0.50).

3.2.2 Effects of Hartmann number

A mathematical study has been executed in this section to examine the effects of Hartmann number (Ha) with different sizes (r = 0.10, 0.20, 0.30 m) of the heated cylinder in the cavity. The investigated results have been shown in terms of streamlines, isotherm lines, average velocity magnitude (V_{av}), average Nusselt number (Nu_{av}) and average fluid temperature (Θ_{av}).

Fig. 3.21 (a-c) explores the streamlines for different Hartmann number with three different sizes of the heated cylinder where CP at (0.50, 0.50), Pr = 0.71, Ra = 10^4. It inquires into in Fig. 3.21 (a-c) that the strength of the velocity magnitude reduces for all sizes of the heated cylinder when the Hartmann number (Ha) is altered from 0 to 50. Streamlines are not found in the right half of the square cavity in Fig. 3.21(c) due to large cylindrical barrier in the cavity The maximum velocity magnitude is 11.09 m/s which is found at the point (0.66, 0.44) when Ha = 0, Pr = 0.71, Ra = 10^4, CP at (0.50, 0.50) and r = 0.10 m.

Fig. 3.22 (a-c) presents the isothermal lines for different Hartmann number with three sizes (r = 0.10, 0.20, 0.30 m) of the heated cylinder in the cavity. When size, r = 0.10 m, some heated isotherms are found between cylinder and heated bottom wall. For larger size (r = 0.30 m) of the cylinder, the isothermal lines are suppressed above the heated cylinder.

Fig. 3.23 exhibits the effects of Prandtl numbers on average velocity magnitude (V_{av}) for different sizes of the heated cylinder, where Pr = 0.71, Ra = 10^4 and CP at (0.50, 0.50). It is observed that the V_{av} decreases with the increase of Hartmann number from 0 to 50. Besides, the V_{av} upturns quickly for the reduction of sizes of the heated cylinder.

Fig. 3.24 displays the effect of Hartmann numbers on average Nusselt number (Nu_{av}) for different sizes of heated cylinder, where Ra = 10^4, Pr = 0.71 and CP at (0.50, 0.50). The Nu_{av} improves slowly when the cylinder size, r = 0.20 and r = 0.30 m. Furthermore, the Nu_{av} for smaller size (r = 0.10 m) of cylinder is always larger compared to the Nu_{av} for medium size (r = 0.20 m). Besides, the Nu_{av} is always superior among the other sizes of the cylinders.

Fig. 3.25 shows the average fluid temperature (Θ_{av}) in the cavity for different sizes of the heated cylinder.

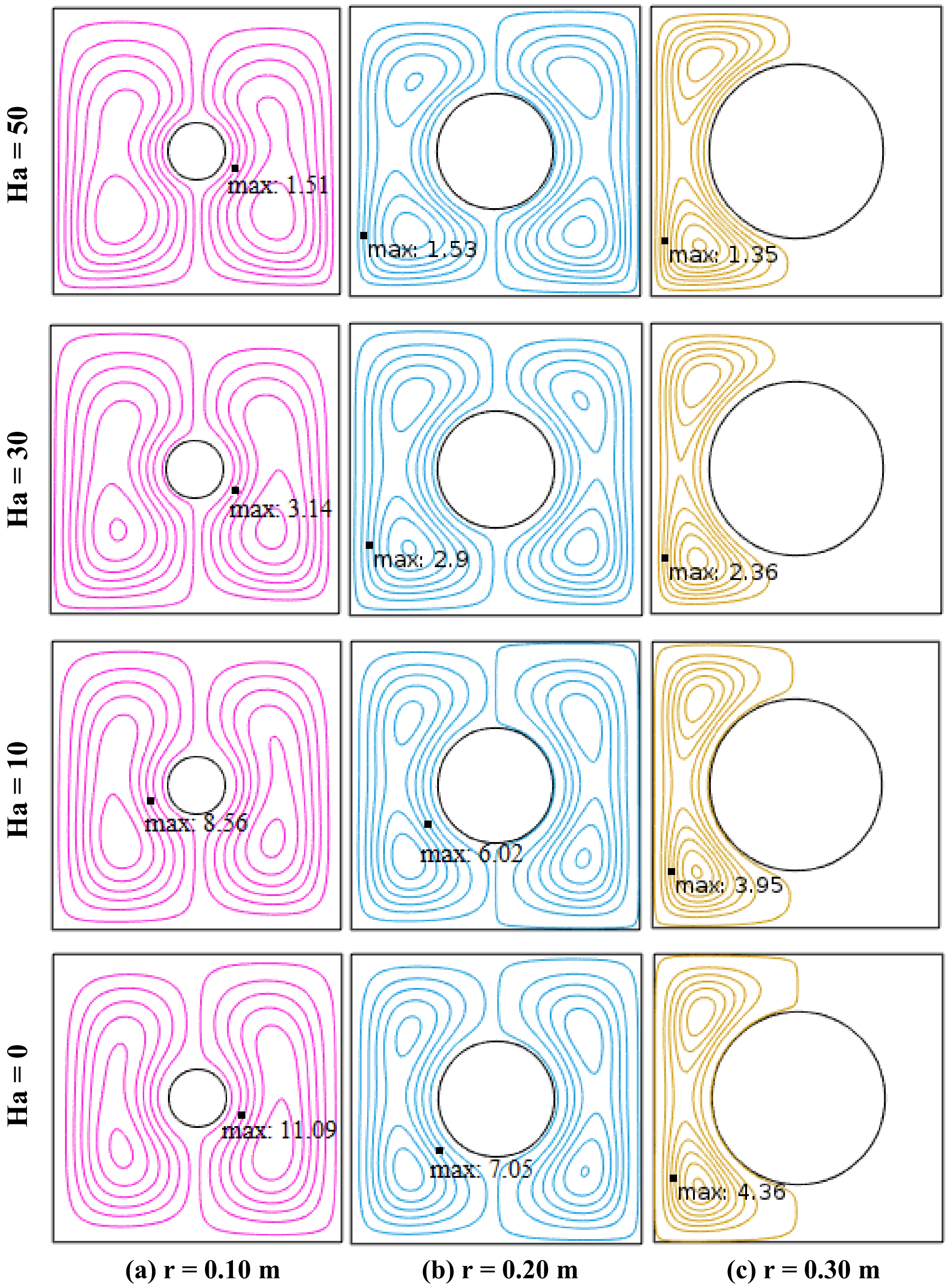

Fig. 3.21 (a-c) Streamlines for different Ha and different sizes of cylinder, where Pr = 0.71 and Ra = 10^4 and CP at (0.50, 0.50).

For all sizes of cylinders, the Θ_{av} reduces very slowly with the increase of Hartmann number from 0 to 50. For large size (r = 0.30 m) of the heated cylinder, the average fluid temperature (Θ_{av}) is larger than the smaller size of cylinder.

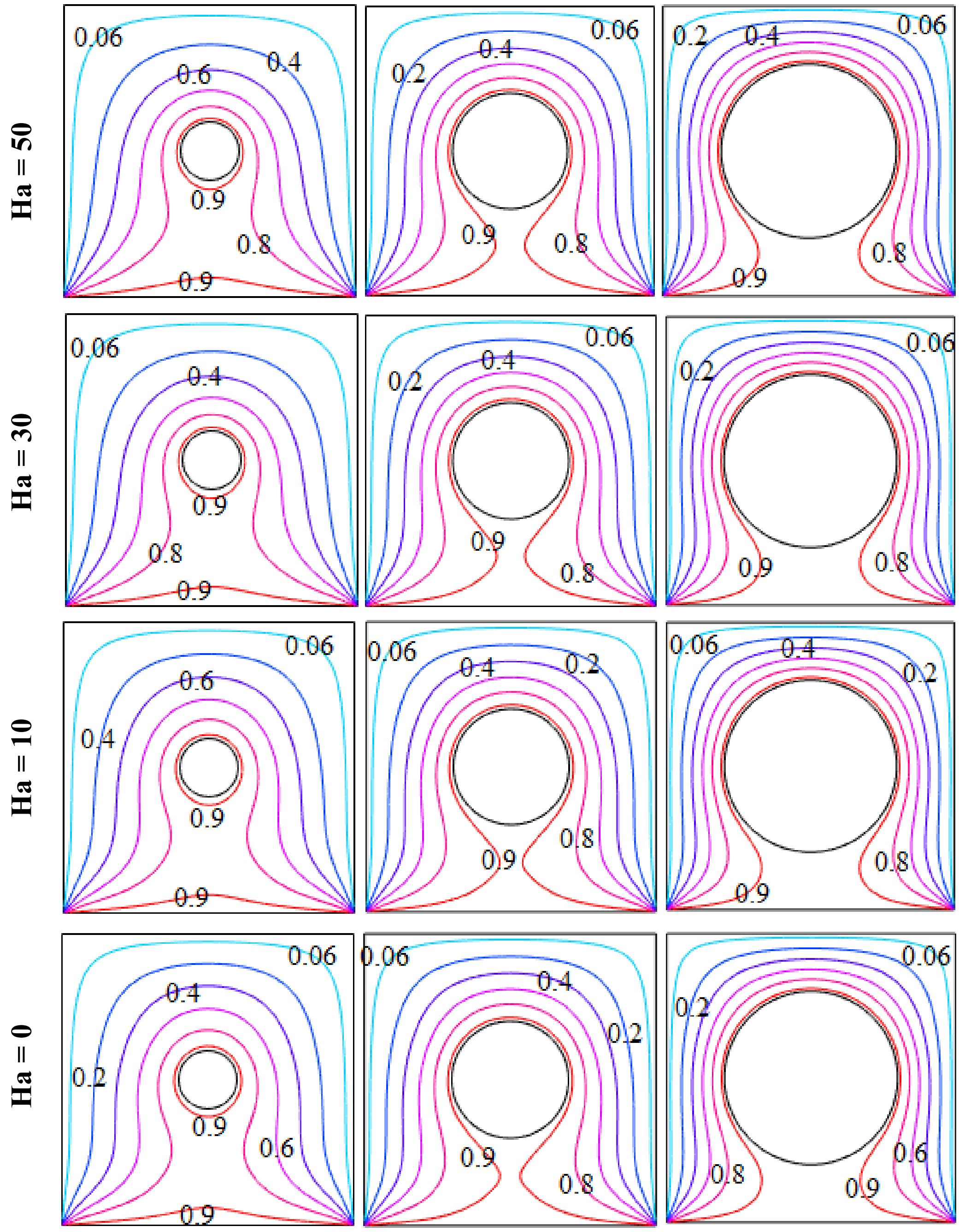

(a) r = 0.10 m **(b) r = 0.20 m** **(c) r = 0.30 m**

Fig. 3.22 (a-c) Isothermal lines for different Ha and different sizes of cylinder, where Pr = 0.71, Ra = 10^4 and CP at (0.50, 0.50).

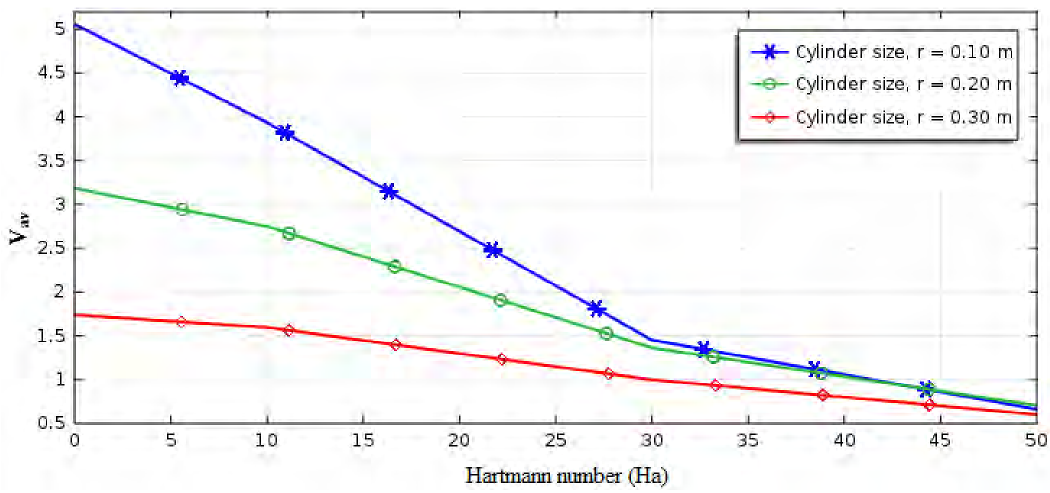

Fig. 3.23 Effect of Hartmann number (Ha) on average velocity magnitude (V_{av}) for different sizes of the cylinder, where Pr = 0.71, Ha = 50 and CP at (0.50, 0.50).

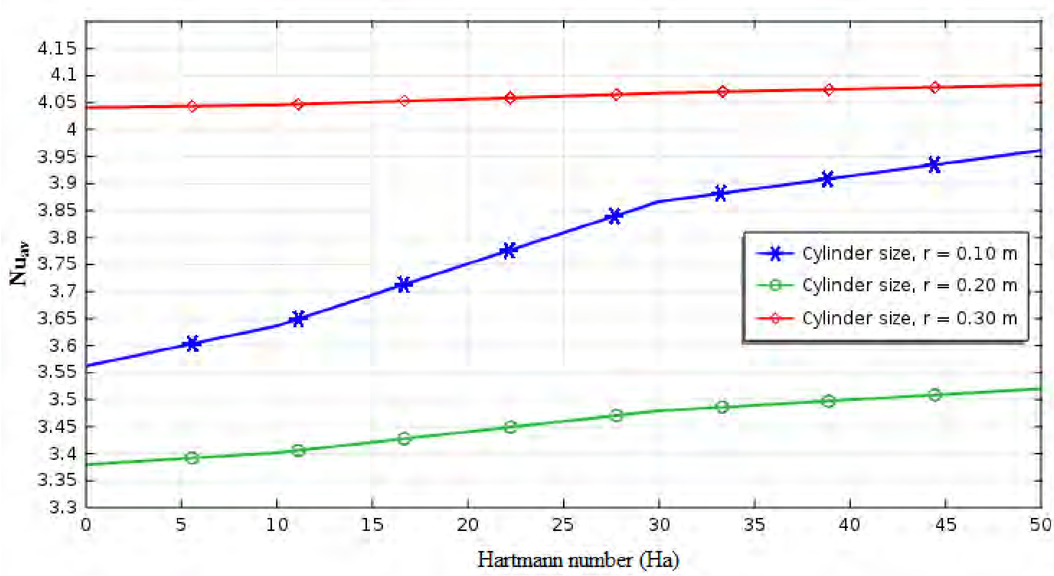

Fig. 3.24 Effect of Hartmann number (Ha) on average Nusselt number (Nu_{av}) for different sizes of the cylinder, where Pr = 0.71, Ra = 10^4 and CP at (0.50, 0.50).

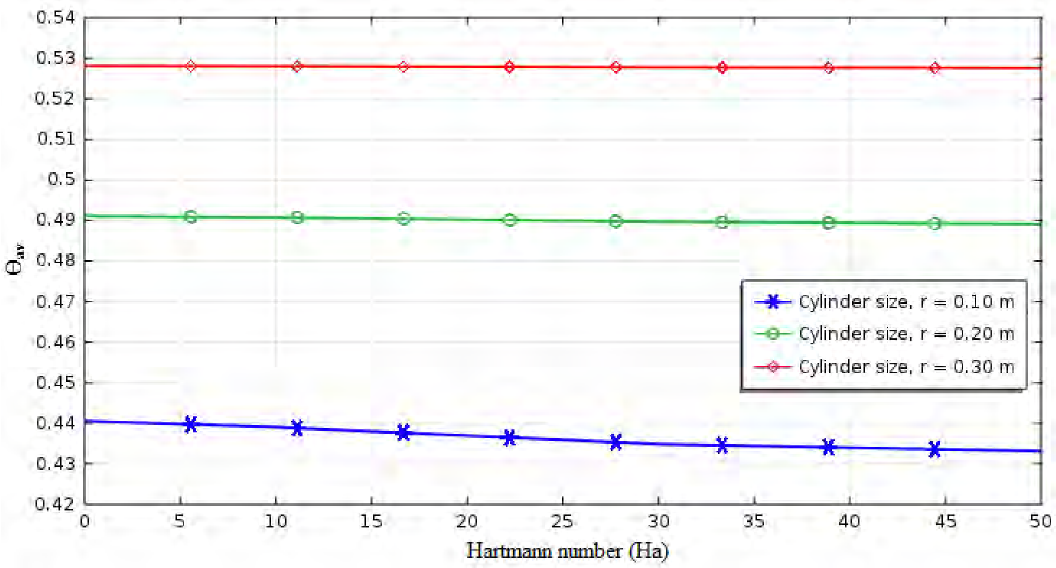

Fig. 3.25 Effect of Hartmann number (Ha) on average fluid temperature (Θ_{av}) for different sizes of the cylinder, where Pr = 0.71, Ra = 10^4 and CP at (0.50, 0.50).

3.2.3 Effects of Prandtl number

The effects of Prandtl number (Pr) for different sizes of heated cylinder on the velocity profile and thermal field in terms of streamlines and isothermal lines have been presented in Fig. 3.26 - 3.27. Fig. 3.26 (a-c) shows the stream lines for different sizes of heated cylinder and different Prandtl numbers from 0.71 to 10. It is viewed that for all sizes of heated cylinder, the strength of the velocity magnitude increase very slowly with the increase of Pr from 0.71 to 10 and the maximum vorticity (3.34 m/s) is observed (0.37, 0.79) for size, r = 0.30 m, Pr = 10, Ha = 50, Ra = 10^4 and CP at (0.50, 0.50).

Fig. 3.27 (a-c) exhibits the isothermal lines for different sizes of heated cylinder and different Prandtl number (Pr). Some heated isothermal contours are found between heated bottom wall and the cylinder in Fig. 3.27 (a). On the other hand, no isothermal lines are not observed between heated bottom wall and the cylinder in Fig. 3.27 (c) because of larger size (r = 0.30 m) of heated cylinder. A few number of isothermal lines are squeezed above the cylinder for large Prandtl number (Pr = 10). For larger size (r = 0.30 m) of the cylinder, all the isothermal lines are concentrated between top wall and the heated cylinder.

Fig. 3.28 shows the effect of Prandtl number (Pr) on average velocity magnitude (V_{av}) for different sizes of the heated cylinder, where Ha = 50, Ra = 10^4 and CP at (0.50, 0.50).

Pr = 10

Pr = 5

Pr = 2

Pr = 0.71

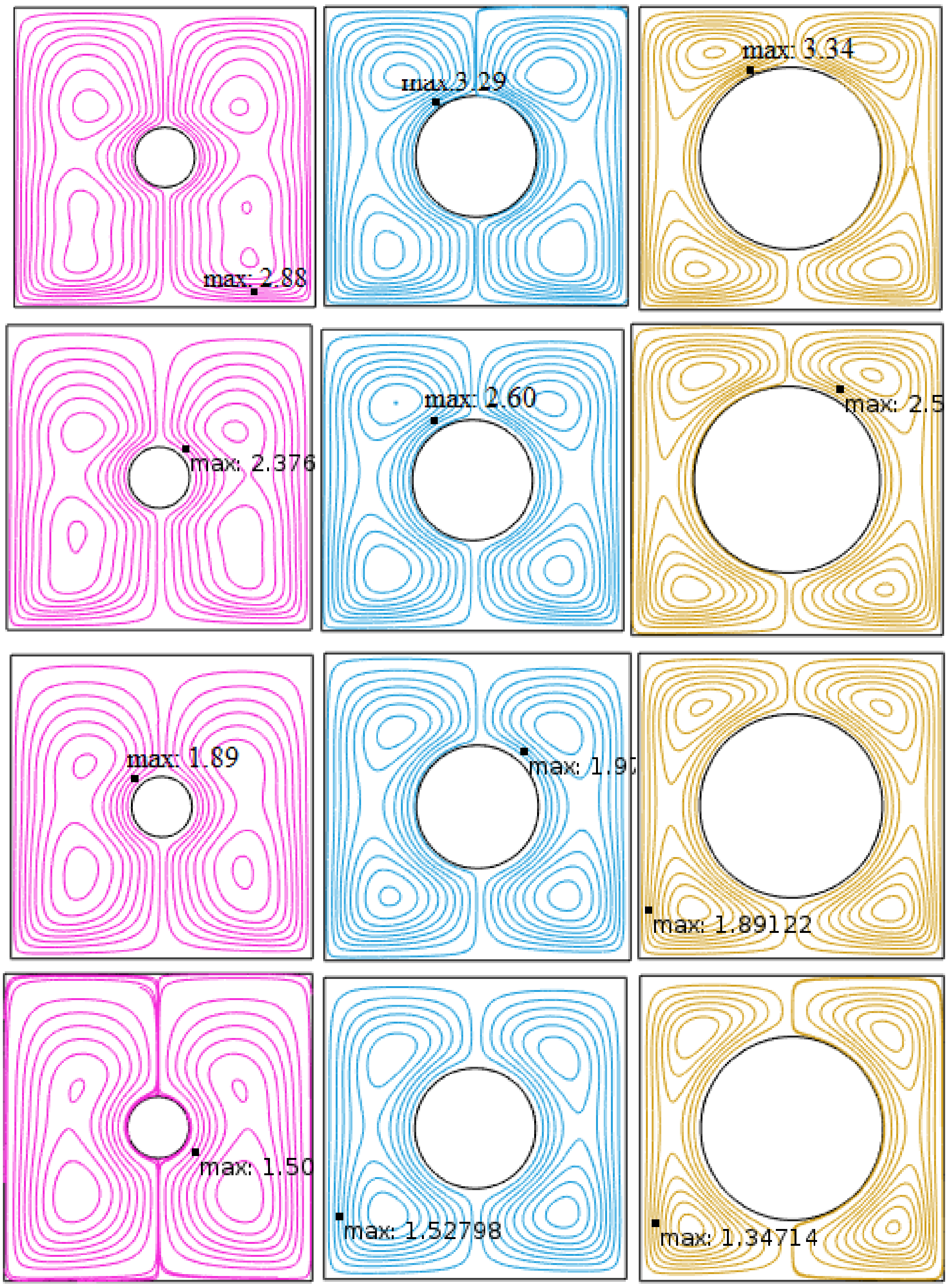

(a) r = 0.10 m **(b) r = 0.20 m** **(c) r = 0.30 m**

Fig. 3.26 (a-c) Streamlines for different Pr and different sizes of cylinder, where Ha = 50, Ra = 10^4 and CP at (0.50, 0.50).

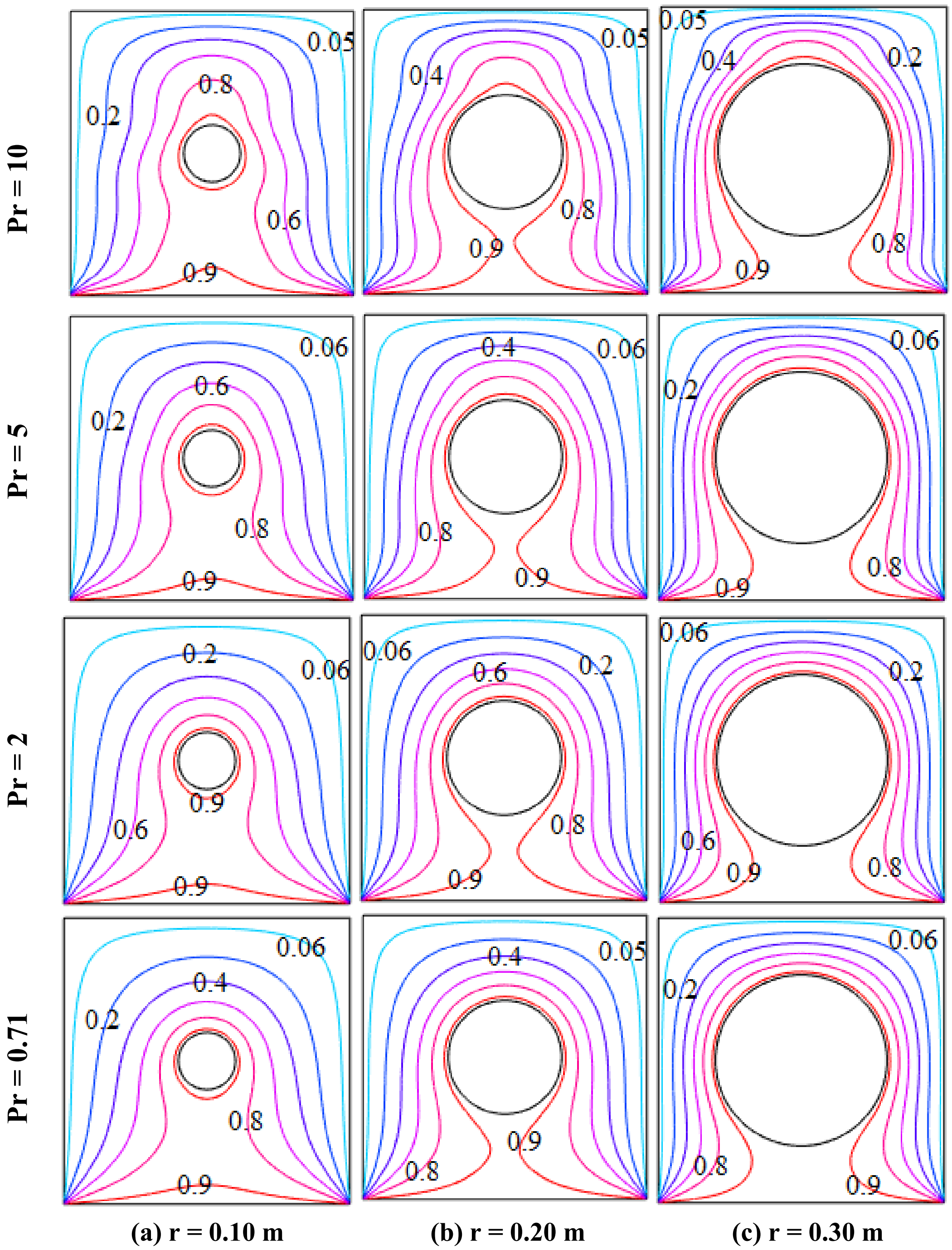

Fig. 3.27 (a-c) Isothermal lines for different Pr and different sizes of cylinder, where Ha = 50, Ra = 10^4, CP at (0.50, 0.50).

For all sizes of the heated cylinders, the V_{av} increases with the increase of Prandtl number from 0.71 to 10. For the larger size (r = 0.30 m) of the cylinder, the V_{av} holds the higher velocity magnitude compare to smaller size when Prandtl number varies from 3.3 to 10.

Fig. 3.29 displays the effect of Prandtl number on Nu_{av} for different sizes of the heated cylinder, where Ha = 50, Ra = 10^4 and CP at (0.50, 0.50). For all sizes of heated cylinder, the Nu_{av} decreases with the increase of Prandtl number from 0.71 to 10. The greatest (4.08) Nu_{av} is found when Pr = 0.71, Ha = 50, Ra = 10^4, size, r = 0.30 m and CP at (0.50, 0.50). Besides, the minimum (3.05) Nu_{av} is viewed when Pr = 10, Ha = 50, Ra = 10^4, size, r = 0.20 m and CP at (0.50, 0.50).

Fig. 3.30 exhibits the effect of Prandtl number on average fluid temperature (Θ_{av}) for different sizes of the heated cylinder where Ha = 50, Ra = 10^4, CP at (0.50, 0.50). The Θ_{av} increases with the increase of Prandtl numbers from 0.71 to 10and for different sizes of the heated cylinders.

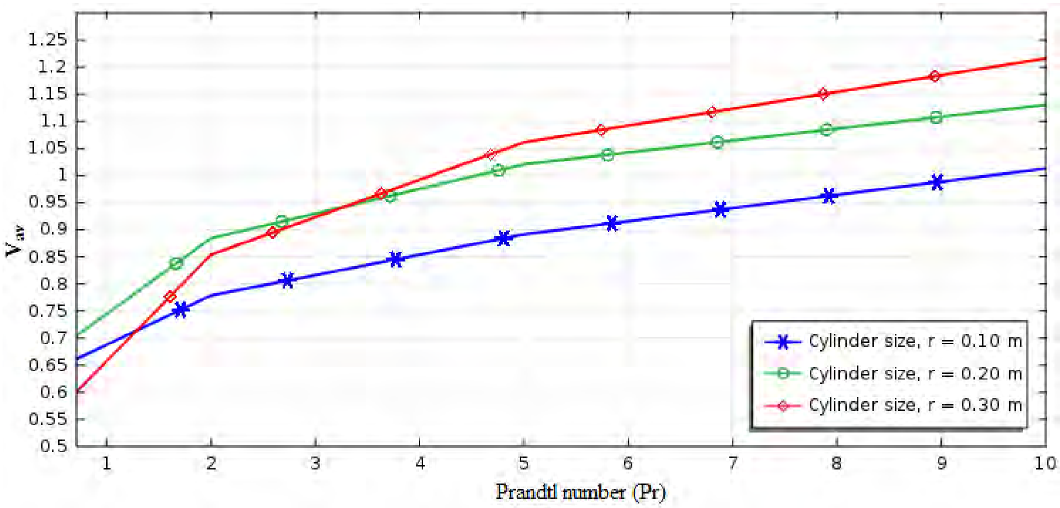

Fig. 3.28 Effect of Prandtl number (Pr) on average velocity magnitude (V_{av}) for different sizes of the cylinder, where Ha = 50, Ra = 10^4 and CP at (0.50, 0.50).

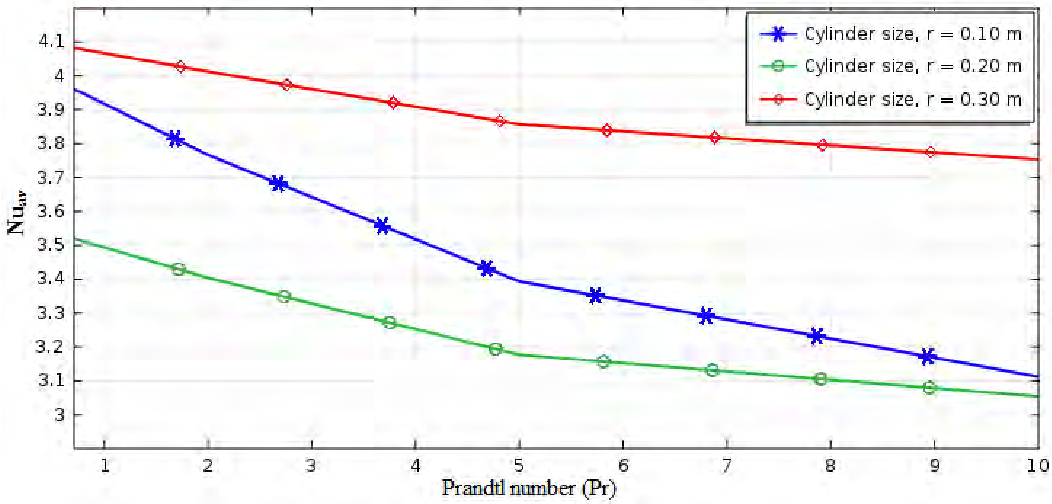

Fig. 3.29 Effect of Prandtl number (Pr) on average Nusselt number (Nu_{av}) for different sizes of the cylinder, where Ha = 50, Ra = 10^4 and CP at (0.50, 0.50).

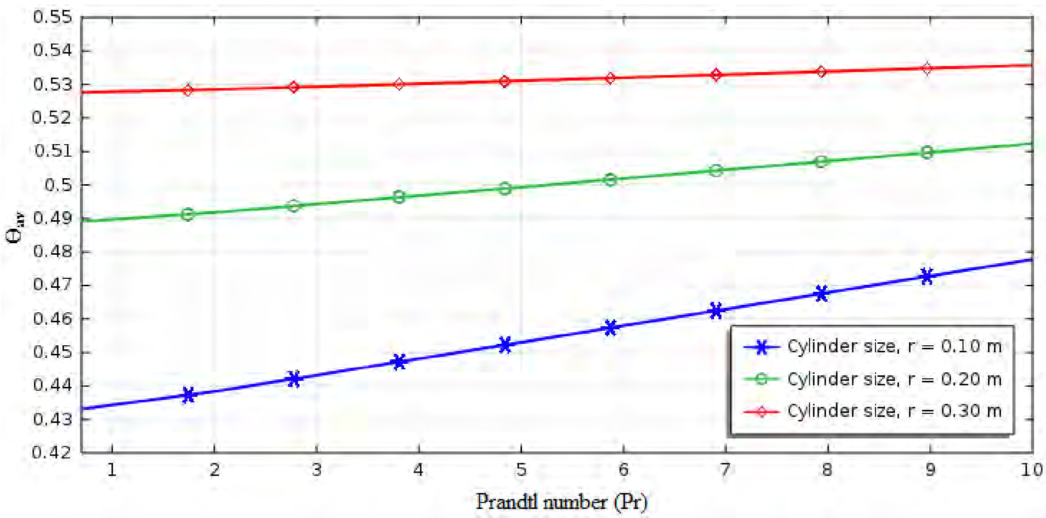

Fig. 3.30 Effect of Prandtl number (Pr) on average fluid temperature (Θ_{av}) for different sizes of the cylinder, where Ha = 50, Ra = 10^4 and CP at (0.50, 0.50).

3.3 Comparative Study

3.3.1 Comparison of Nu_{av} between with and without cylinder

Comparison of average Nusselt numbers (Nu_{av}) along the heated bottom wall of the cavity in the absence of heated cylinder and in the presence of heated cylinder have been investigated in Table 3.1 where Pr = 0.71, CP at (0.50, 0.50), r = 0.20 m and Ra = 10^4 to 5×10^6.It is observed that the Nu_{av} increases for Ha = 0 to 50 and different Rayleigh numbers (Ra = 10^4 to 5×10^6) for both cases. The largest (17.47) Nu_{av} is obtained when Pr = 0.71, Ra = 5×10^6, Ha = 10 and the absence of heated cylinder. For low Rayleigh number (Ra = 10^4 to 10^5), the Nu_{av} decreases with the increase of Hartmann number from 0 to 50 for both cases.

Pr = 0.71	Average Nusselt Number (Nu_{av}) (along the heated bottom wall)					
Ra	Heat flow without heated cylinder			Heat flow with heated cylinder (r = 0.20 m)		
	Ha = 0	10	50	Ha = 0	10	50
10^4	5.92	5.75	5.56	5.01	4.97	4.79
10^5	8.03	7.94	5.91	7.53	7.29	5.47
10^6	11.68	12.05	10.34	11.34	11.92	10.07
5×10^6	16.35	17.47	15.15	16.21	16.83	15.04

Table 3.1 Comparison of average Nusselt number (Nu_{av}) along the heated bottom wall between with and without heated cylinder of the cavity, where r = 0.20 m, Pr = 0.71 and CP at (0.50, 0.50).

3.3.2 Comparison of V_{av} between with and without cylinder

The average velocity magnitude (V_{av}) has been presented for two cases in Table 3.2, (a) In the absence of heated cylinder and (b) In the presence of heated cylinder. For low Rayleigh number (Ra = 10^4 to10^5), the V_{av} declines for both cases. The largest average velocity magnitude (396.63 m/s) is found when Ra = 5×10^6, Ha = 0, Pr = 0.71 and the heated cylinder is absent in the cavity. Besides, the maximum average velocity magnitude (253.77 m/s) is viewed when Ra = 5×10^6, Ha = 10, Pr = 0.71 and the heated cylinder (r = 0.20 m) is present in the cavity. Therefore, V_{av} has affected more in the absence of any barrier in the cavity.

Pr = 0.71	Average velocity magnitude (V_{av}) in the cavity					
Ra	(a) Heat flow without heated cylinder			(b) Heat flow with heated cylinder (r = 0.20 m)		
	Ha = 0	10	50	Ha = 0	10	50
10^4	6.59	4.12	0.43	2.79	2.40	0.62
10^5	43.10	34.96	5.54	27.03	24.37	6.62
10^6	167.67	140.19	50.76	102.29	113.26	56.51
5×10^6	396.63	292.43	123.72	235.37	253.77	146.22

Table 3.2 Comparison of average velocity magnitude (V_{av}) in the cavity with and without heated cylinder, where r = 0.20 m, Pr = 0.71 and position of the cylinder at (0.50, 0.50).

3.3.3 Comparison among present result and previous studies

The present results are verified against the existing results available in the literature. Table 3.3 shows the average Nusselt number (Nu_{av}) of present research compared to other published researches with errors. It exhibits the Nu_{av} of three different researches along the heated bottom wall of the cavity. It has been observed from Table 3.3 that a good agreement is found among the published results with the present research except for Ra = 10^5, Ha = 100.

Ra	Ha	Average Nusselt number (Nu_{av})			% of error	
		Pirmohammadi *et al.* (2008)	Jani *et al.* (2013)	Present research	Pirmohammadi *et al.* (2008)	Jani *et al.* (2013)
10^4	0	2.29	2.289	2.30163	0.51	0.55
	50	1.06	1.061	1.05602	0.38	0.47
	100	1.02	1.019	1.00862	1.12	1.02
10^5	0	4.62	4.631	4.63630	0.35	0.11
	25	3.51	3.507	3.56274	1.50	1.59
	100	1.37	1.365	1.23540	9.82	9.49

Table 3.3 Comparison of average Nusselt number (Nu_{av}) among present result and previous studies.

CHAPTER 4

CONCLUSIONS

The effects of cylinder position and size on MHD natural convection flow in a square cavity have been performed by solving continuity equation, momentum equations and energy equation numerically. The results are presented for flow and thermal fields as well as heat transfer for different positions and sizes of the heated cylinder. A constant hot temperature (T_h) is taken at the bottom wall of the cavity and cylinder while the remaining side walls are kept at cold temperature (T_c) for both the cases. Weighted residual Finite Element method has been used to solve the governing equations. Comparisons with the published work is performed and found to be in a good agreement. The various ideas and results have been discussed in detail in the relevant chapters in this thesis. The overall research can be summed up through the subsequent conclusions.

4.1 Summary of the Major Outcomes

Two different cases as case I (Variation of cylinder's position) and case II (Variation of cylinder size) have been illustrated in this research. On the basis of the analysis the following conclusions are drawn.

4.1.1 Case I: Variation of cylinder's position

- ✓ The maximum strength of the velocity magnitude (460.6 m/s) is obtained at (0.50, 0.20) for Ra = 5×10^6 when CP at (0.50, 0.75), size of the cylinder, r = 0.20 m, Pr = 0.71 and Ha = 50.
- ✓ The greatest average velocity magnitude (167 m/s) is found for CP at (0.50, 0.50), Ra = 5×10^6, Pr = 0.71, Ha = 50 and size of the cylinder, r = 0.20 m.
- ✓ The average Nusselt number (Nu_{av}) along the heated cylinder is maximum (9.6) when CP at (0.50, 0.75), Ra = 5×10^6, Pr = 0.71, Ha = 50, cylinder size, r

= 0.20 m and is minimum (2.355) when CP at (0.50, 0.25), Ra = 10^4, Pr = 0.71, Ha = 50, cylinder size, r = 0.20 m.

- ✓ The rate of heat transfer is increased approximately 130.2% for Ra variation, 13.4% for Pr variation and decreased as 4.1% for Ha variation when the cylinder size, r = 0.20 m, and CP at (0.50, 0.50).
- ✓ The average fluid temperature (Θ_{av}) of the cavity is maximum (0.53) when CP at (0.50, 0.75) where Pr = 10, Ha = 50, Ra = 104, r = 0.20 m and minimum (0.377) when Ra = 10^4, Ha = 50, Pr = 0.71, r = 0.20 m, CP at (0.50, 0.25).

4.1.2 Case II: Variation of cylinder size

In this case, the cylinder is kept at centre of the cavity and alters the sizes of the cylinder. Streamlines, isotherms, average velocity magnitude (V_{av}), average Nusselt number (Nu_{av}), and average fluid temperature (Θ_{av}) as well as characteristics of heat transfer process particularly its expansion has been evaluated in chapter 3 (Case II). On the basis of the analysis the following conclusions have been drawn:

- ✓ The maximum strength (466.4 m/s) of the velocity magnitude is obtained at (0.50, 0.24) when Ra = 5×10^6, cylinder size, r = 0.10 m, Pr = 0.71 and Ha = 50.
- ✓ The greatest average velocity magnitude (184 m/s) is found for CP at (0.50, 0.50), Ra = 5×10^6, Pr = 0.71, Ha = 50 and size, r = 0.30 m.
- ✓ The average Nusselt number (Nu_{av}) along the heated cylinder is maximum (10.7) when cylinder size, r = 0.10 m, Ra = 5×10^6, Pr = 0.71, Ha = 50, CP at (0.50, 0.50), and is minimum (3.05) when cylinder size, r = 0.20 m, Ra = 10^4, Pr = 0.71, Ha = 50, CP at (0.50, 0.50).
- ✓ The rate of heat transfer is increased approximately 170.9% for Ra variation, 21.5% for Pr variation and decreased as 11.2% for Ha variation when the cylinder size, r = 0.10 m, and CP at (0.50, 0.50).

- ✓ The average fluid temperature (Θ_{av}) of the cavity is maximum (0.536) for Pr = 10, r = 0.30 m, Ha = 50, Ra = 10^4, CP at (0.50, 0.50), and minimum (0.433) for r = 0.10 m, Pr = 0.71, Ra = 10^4, Ha = 50, Pr = 0.71 and cylinder position is at (0.50, 0.50).
- ✓ The heat transfer rate is more affected for the size variation of the heated cylinder compare to the position variation.

4.2 Extension of this research

In consideration of the present investigation "Effects of cylinder location and size on MHD natural convection flow in a square cavity", the following recommendations for future works may be provided.

- MHD natural convection with two heated cylinders inside a square cavity using weighted residual Finite Element method.
- Heat transfer analysis in a square cavity heated from the top and bottom walls with MHD natural convection flow.
- Effect of conduction on MHD free convection heat flow in a square cavity with a square cylindrical block.
- Effects of various locations of a cylinder on MHD natural convection flow in a square cavity
- Mixed and forced convection can also be considered to the governing equations of concentration conservation.
- Two-dimensional fluid flow and heat transfer has been analyzed in this thesis. So this reflection may be extended to three-dimensional analyses to explore the effects of parameters on flow fields and heat transfer in cavities. In addition, the problem of fluid flow and heat transfer along with heat generating cylinder may be studied in three-dimensional cases.

REFERENCES

Alam M.S., Mollah M.S.H., Alim M.A., Kabir M.K.H., "Finite element analysis of MHD natural convection in a rectangular cavity and partially heated wall", Eng. Appl. Sci., vol. 2, no. 3, pp. 53-58, 2017.

Ali M.M., Alim M.A., Maleque M.A. and Ahmed S.S., "Numerical simulation of MHD free convection flow in a differentially heated square enclosure with tilted obstacle", AIP Conf. Proc., vol. 1851, pp. 020055(1-8), 2017.

Ashouri M., Shafii M.B., and Kokande H.R. "MHD natural convection flow in cavities filled with square solid blocks", Int. J. Numerical Methods Heat Fluid Flow, vol. 24, no. 8, pp. 1813-1830, 2014.

Aydin O., Ünal A. and Ayhan T., "Natural convection in rectangular enclosures heated from one side and cooled from the ceiling", Int. J. of Heat and Mass Transfer, vol. 42, pp. 2345-2355, 1999.

Bakar N.A., Karimipour A., and Roslan R., "Effect of magnetic field on mixed convection heat transfer in a lid-driven square cavity", J. of Therm., vol. 2016, pp. 1-14, 2016.

Basak T., Roy S., and Pop I., "Heat flow analysis for natural convection within trapezoidal enclosures based on heatline concept", Int. J. Heat Mass Transf., vol. 52, pp. 2471-2483, 2009.

Basak T., Roy S., Singh S.K., and Pop I., "Analysis of mixed convection in a lid-driven porous square cavity with linearly heated side wall(s)", Int. J. Heat Mass Transf., vol. 53, pp. 1819-1840, 2010.

Bejan A, "Convection Heat Transfer", John Wiley & Sons, Hoboken, New Jersey, 4th ed., Book Review, pp. 1-690, 2013.

Bouabid M., Magherbi M., Hidouri N. and Brahim A.B., “Entropy generation at natural convection in an inclined rectangular cavity”, Entropy, vol. 13, no. 5, pp. 1020-1033, 2011.

Chamkha A.J., Hussain S.H., and Abd-Amer Q.R., “Mixed convection heat transfer of air inside a square vented cavity with a heated horizontal square cylinder”, Numerical Heat Transf. Part A Appl., vol. 59, pp. 58-79, 2011.

Ece M.C. and Büyük E., “Natural-convection flow under a magnetic field in an inclined rectangular enclosure heated and cooled on adjacent walls”, Fluid Dynamics Research, vol. 38, pp. 564-590, 2006.

Gangawane K.M. and Bharti R.P., “Computational analysis of magnetohydrodyna mic natural convection in partially differentially heated cavity: Effect of cooler size”, Proc IMechE Part C, J. Mechanical Engineering Science, vol. 232(3), pp. 515-528, 2018.

Ganzarolli M.M. and Milanez L.F., “Natural convection in rectangular enclosures heated from below and symmetrically cooled from the sides”, Int. J. Heat Mass Transfer, vol. 38, no. 6, pp. 1063-1073, 1995.

Hamama O.S.K., Sharif F.S., and Hidouri M.N., “Irreversibility investigation on MHD natural convection in a square cavity for different Prandtl numbers”, vol. 3, no. 4, pp. 90-104, 2016.

Han C.Y., “Hydro-magnetic free convection of a radiating fluid”, Int. J. Heat Mass Transf., vol. 52, pp. 5895-5908, 2009.

Hasanuzzaman M., Öztop H.F., Rahman M.M., Rahim N.A., Saidur R., and Varol Y., “Magnetohydrodynamic natural convection in trapezoidal cavities”, Int. Commu nication Heat Mass Transf., vol. 39, no. 9, pp. 1384-1394, 2012.

Hossain M.A. and Wilson M., “Natural convection flow in a fluid-saturated porous medium enclosed by non-isothermal walls with heat generation”, Int. J. Therm. Sci., vol. 41, no. 5, pp. 447-454, 2002.

Hossain S.A, Alim M.A. and Saha S.K., “A finite element analysis on MHD free convection flow in open square cavity containing heated circular cylinder”, American J. of Computational Mathematics, vol. 5, pp. 41-54, 2015.

Hossain S.A, Alim M.A., and Saha S.K., “Effect of Prandtl number and inclination angle on MHD natural convection in inclined open square cavity,” Phys. Sci. Int. J., vol. 14, no. 4, pp. 1-13, 2017.

Jalil J.M., Al-Tae’y K.A., and Ismail S.J., “Natural convection in an enclosure with a partially active magnetic field”, Numerical Heat Transf. Part A Appl., vol. 64, no. 1, pp. 72-91, 2013.

Jami M., Mezrhab A. and Naji H., “Numerical study of natural convection in a square cavity containing a cylinder using the lattice Boltzmann method”, Int. J. for Computer Aided Eng. and Software, vol. 25, no. 5, pp. 480-489, 2008.

Jani S., Mahmoodi M., and Amini M., “Magnetohydrodynamic free convection in a square cavity heated from below and cooled from other”, World Academy of Science, Engineering and Technology, vol. 7, no. 4, pp. 329-334, 2013.

Javed T., Siddiqui M.A., and Mehmood Z., “MHD natural convective flow through a porous medium in a square cavity filled with liquid gallium”, Thermo physics Aeromechanics, vol. 25, no. 3, pp. 405-420, 2018.

Kahveci K. and Öztuna S., “MHD natural convection flow and heat transfer in a laterally heated partitioned enclosure”, Eur. J. Mech. B/Fluids, vol. 28, no. 6, pp. 744-752, 2009.

Kahveci K., “Numerical simulation of natural convection in a partitioned enclosure using PDQ method”, Int. J. Numerical Methods Heat Fluid Flow, vol. 17, no. 4, pp. 439-456, 2007.

Kakarantzas S.C., Sarris I.E., and Vlachos N.S., “MHD natural convection of liquid metal between coaxial isothermal cylinders due to internal heating”, Numerical Heat Transf. Part A Appl., vol. 65, no. 5, pp. 401-418, 2014.

Kakarantzas S.C., Sarris I.E., Grecos A.P., and Vlachos N.S., "Magnetohydrodyna mic natural convection in a vertical cylindrical cavity with sinusoidal upper wall temperature", Int. J. Heat Mass Transf., vol. 52, pp. 250-259, 2009.

Kherief N.M. Berrahil F. and Talbi K., "Magneto-hydrodynamic flow in a two-dimensional inclined rectangular enclosure heated and cooled on adjacent walls", J. of Applied Fluid Mechanics, vol. 9, no. 1, pp. 205-213, 2016.

Kim B.S., Lee D.S., Ha M.Y., and Yoon H.S., "A numerical study of natural convection in a square enclosure with a circular cylinder at different vertical locations," Int. J. Heat Mass Transf., vol. 51, pp. 1888-1906, 2008.

Kim M., Doo J.H., Park Y.G., Yoon H.S. and Ha M.Y., "Natural convection in a square enclosure with a circular cylinder with adiabatic side walls according to bottom wall temperature variation", J. Mech. Sci. Technol., vol. 32, no. 7, pp. 3201-3211, 2014.

Luo X.H., Li B.W., and Hu Z.M., "Effects of thermal radiation on MHD flow and heat transfer in a cubic cavity", Int. J. Heat Mass Transf., vol. 92, pp. 449-466, 2016.

Mahmud S. and Fraser R.A., "Magnetohydrodynamic free convection and entropy generation in a square porous cavity", Int. J. Heat Mass Transf., vol. 47, pp. 3245-3256, 2004.

Munshi M.J.H., Alim M.A., Bhuiyan A.H., and Mostafa G., "Effect of a Magneto-hydrodynamic natural convection in a square cavity with elliptic shape adiabatic block", American J. of Eng. Research (AJER), vol. 4, pp. 10-22, 2015.

Obayedullah M. and Chowdhury M.M.K., "MHD natural convection in a rectangular cavity having internal energy sources with non-uniformly heated bottom wall", Procedia Eng., vol. 56, pp. 76-81, 2013.

Oztop H.F., Al-Salem K., and Pop I., "MHD mixed convection in a lid-driven cavity with corner heater", Int. J. Heat Mass Transf., vol. 54, pp. 3494-3504, 2011.

Park Y.G., Ha M.Y., and Yoon H.S., “Study on natural convection in a cold square enclosure with a pair of hot horizontal cylinders positioned at different vertical locations”, Int. J. Heat Mass Transf., vol. 65, pp. 696-712, 2013.

Park Y.G., Ha M.Y., Choi C., and Park J., “Natural convection in a square enclosure with two inner circular cylinders positioned at different vertical locations”, Int. J. Heat Mass Transf., vol. 77, pp. 501-518, 2014.

Pirmohammadi M., Ghassemi M. and Sheikhzadeh G.A., “The effect of a magnetic field on buoyancy-driven convection in differentially heated square cavity”, Institute of Electrical and Electronics Engineers (IEEE), vol. 6, pp. 1-6, 2008.

Pirmohammadi M. and Ghassemi M., “Effect of magnetic field on convection heat transfer inside a tilted square enclosure”, Int. Communication Heat Mass Transf., vol. 36, no. 7, pp. 776-780, 2009.

Rahman M.M., Alim M.A., and Chowdhury M.K., “Magnetohydrodynamics mixed convection around a heat conducting horizontal circular cylinder in a rectangular lid-driven cavity with joule heating,” J. Sci. Res., vol. 1, no. 3, pp. 461-472, 2009.

Rahman M.M., Alim M.A., and Sarker M.M.A., “Numerical study on the conjugate effect of joule heating and magneto-hydrodynamics mixed convection in an obstructed lid-driven square cavity”, Int. Communication Heat Mass Transf., vol. 37, no. 5, pp. 524-534, 2010.

Rahman M.M., Mamun M.A.H., and Saidur R., “Analysis of magnetohydrodynamic mixed convection and joule heating in lid-driven cavity having a square block”, J. Chinese Inst. Eng. Trans. Chinese Inst. Engineering A/Chung-kuo K. Ch’eng Hsuch K’an, vol. 34, no. 5, pp. 585-599, 2011.

Roslan R., Saleh H., and Hashim I., “Natural convection in a differentially heated square enclosure with a solid polygon”, Sci. World J., vol. 2014, pp. 1-11, 2014.

Saha S.C., “Effect of MHD and heat generation on natural convection flow in an open square cavity under microgravity condition”, Engineering Computation (Swansea, Wales), vol. 30, no. 1, pp. 5-20, 2013.

Sathiyamoorthy M. and Chamkha A.J., "Natural convection flow under magnetic field in a square cavity for uniformly (or) linearly heated adjacent walls", Int. J. Numerical Methods Heat Fluid Flow, vol. 22, no. 5, pp. 677-698, 2012.

Sathiyamoorthy M. and Chamkha A., "Effect of magnetic field on natural convection flow in a liquid gallium filled square cavity for linearly heated side wall(s)", Int. J. Therm. Sci., vol. 49, no. 9, pp. 1856-1865, 2010.

Sathiyamoorthy M., Basak T., Roy S., and Pop I., "Steady natural convection flows in a square cavity with linearly heated side wall(s)", Int. J. Heat Mass Transf., vol. 50, pp. 766-775, 2007.

Sheikhzadeh G.A., Fattahi A., Mehrabian M.A., and Pirmohammadi M., "Effect of geometry on magneto-convection in a square enclosure filled with a low Prandtl number fluid", Proc. Inst. Mech. Eng. Part E J. Process Mech. Eng., vol. 225, no. 1, pp. 53-61, 2010.

Turk Ö., and Sezgin M.T., "FEM solution of natural convection flow in square enclosures under magnetic field", Int. J. Numerical Methods Heat Fluid Flow, vol. 23, no. 5, pp. 844-866, 2013.

Varol Y., Oztop H.F., and Pop I., "Conjugate heat transfer in porous triangular enclosures with thick bottom wall", Int. J. Numerical Methods Heat Fluid Flow, vol. 19, no. 5, pp. 650-664, 2009.

Zhang P., Zhang X., Deng J., and Song L., "A numerical study of natural convection in an inclined square enclosure with an elliptic cylinder using variational multi-scale element free Galerkin method", Int. J. Heat Mass Transf., vol. 99, pp. 721-737, 2016.

Zienkiewicz O.C. and Taylor R.L., "The finite element method", McGrow-Hill, vol. 2, pp. 1-648, 1989.